I&EC research
Industrial & Engineering Chemistry Research

pubs.acs.org/IECR

Article

Electroreduction of CO_2/CO to C_2 Products: Process Modeling, Downstream Separation, System Integration, and Economic Analysis

Mahinder Ramdin,* Bert De Mot, Andrew R. T. Morrison, Tom Breugelmans, Leo J. P. van den Broeke, J. P. Martin Trusler, Ruud Kortlever, Wiebren de Jong, Othonas A. Moultos, Penny Xiao, Paul A. Webley, and Thijs J. H. Vlugt

Cite This: https://doi.org/10.1021/acs.iecr.1c03592

Read Online

ACCESS | Metrics & More | Article Recommendations | Supporting Information

ABSTRACT: Direct electrochemical reduction of CO_2 to C_2 products such as ethylene is more efficient in alkaline media, but it suffers from parasitic loss of reactants due to (bi)carbonate formation. A two-step process where the CO_2 is first electrochemically reduced to CO and subsequently converted to desired C_2 products has the potential to overcome the limitations posed by direct CO_2 electroreduction. In this study, we investigated the technical and economic feasibility of the direct and indirect CO_2 conversion routes to C_2 products. For the indirect route, CO_2 to CO conversion in a high temperature solid oxide electrolysis cell (SOEC) or a low temperature electrolyzer has been considered. The product distribution, conversion, selectivities, current densities, and cell potentials are different for both CO_2 conversion routes, which affects the downstream processing and the economics. A detailed process design and techno-economic analysis of both CO_2 conversion pathways are presented, which includes CO_2 capture, CO_2 (and CO) conversion, CO_2 (and CO) recycling, and product separation. Our economic analysis shows that both conversion routes are not profitable under the base case scenario, but the economics can be improved significantly by reducing the cell voltage, the capital cost of the electrolyzers, and the electricity price. For both routes, a cell voltage of 2.5 V, a capital cost of \$10,000/m^2, and an electricity price of <\$20/MWh will yield a positive net present value and payback times of less than 15 years. Overall, the high temperature (SOEC-based) two-step conversion process has a greater potential for scale-up than the direct electrochemical conversion route. Strategies for integrating the electrochemical CO_2/CO conversion process into the existing gas and oil infrastructure are outlined. Current barriers for industrialization of CO_2 electrolyzers and possible solutions are discussed as well.

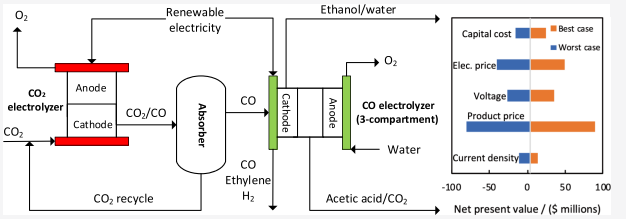

INTRODUCTION

In the past decade, electrochemical reduction of CO_2 (CO2R) to C_1 products (e.g., CO and formic acid) has been studied extensively.[1−3] The outcome of all these efforts is that CO and formic acid/formate can be produced with high Faraday efficiencies (FEs > 90%) and industrial scale current densities (CDs > 150 mA/cm^2), but only in near-neutral to alkaline pH conditions. Recent studies show that CO2R to C_{2+} products such as ethylene and acetic acid/acetate are also favored in alkaline media. The selectivity of the existing (copper-based) catalysts for C_{2+} products is significantly lower than that for C_1 products, which results in a mixture of several (by)products. Although CO2R in alkaline media seems to be promising in terms of FEs, it has some major drawbacks, which significantly affects the economics and scale-up of CO_2 electrolyzers. For example, CO2R to ethylene in alkaline media can be represented by the following reaction:

$$2CO_2 + 8H_2O + 12e^- \rightarrow C_2H_4 + 12OH^- \quad (1)$$

Note that eq 1 is often written in acidic form (i.e., a proton (H^+) instead of water is used as a hydrogen source), even though the reaction is performed in alkaline media. In this way, the formation of hydroxide ions, which forms the basis for all the problems in alkaline CO_2 electrolysis, is eliminated from the reaction. The reaction should be written in alkaline form, not only to be consistent with the pH conditions, but also due to the fact that water and not H^+ is involved in the CO2R mechanism, as ascertained by Hori.[4] The drawbacks of CO2R in alkaline conditions are related to the formed hydroxide ions, which react with fresh CO_2 supplied to the cathode resulting in (bi)carbonate precipitation in gas diffusion electrodes (GDEs). A large fraction of the supplied CO_2 is converted to (bi)carbonate, which has a dramatic effect on the CO_2 utilization efficiency.[5] In the best case, 12 mol of CO_2 is converted to (bi)carbonate for every mole of ethylene obtained. In practice, more CO_2 will be converted to (bi)carbonate, because part of the CO_2 also reacts with the

Received: September 5, 2021
Revised: November 18, 2021
Accepted: November 18, 2021

alkaline electrolyte. It is difficult to avoid CO_2 losses in alkaline solutions, because the absorption rate of CO_2 in concentrated potassium or sodium hydroxide (KOH or NaOH) is much higher than the electrochemical conversion rate of CO_2. For example, the initial absorption rate of CO_2 in a 7 M KOH solution is around 6 sccm/cm^2,[6] which is a factor of 10 faster than the electrochemical conversion rate of CO_2 to ethylene at 250 mA/cm^2. Furthermore, in alkaline solutions, weak acids such as formic acid or acetic acid almost completely dissociate into the ionic form, which is not the desired product from a market perspective and complicates the downstream processing.[7] A simple solution would be to perform the CO2R in (slightly) acidic conditions, but the Faraday efficiency tends to be lower, because the competing hydrogen evolution reaction (HER) is dominant in low pH solutions.[8,9] Recently, Huang et al.[10] achieved promising results for CO_2 electrolysis to multicarbon products in very acidic solutions, but this approach is still in its infancy and needs to be developed further. An alternative solution is to use a three-compartment cell, where CO_2 is reduced in the cathode compartment, water is oxidized in the anode compartment, and protons from the anode and the conjugate bases (e.g., formate, acetate, bicarbonate) from the cathode are combined in the center compartment to produce acids.[11] However, the combination of protons and bicarbonate ions will cause CO_2 evolution in the center compartment, which might result in a potential drop. In addition, the center compartment needs to be filled up with an ion conducting material, because the conductivity of undissociated acids is poor. Therefore, the capital (CAPEX) and operating (OPEX) costs of a three-compartment CO_2 electrolyzer will be higher due to the increased complexity and higher potential requirement. Another option is to convert (bi)carbonate to chemicals using bipolar membrane (BPM) based electrochemical cells, but the potential of this route has yet to be explored.[12−14] Recently, Lee et al.[15] showed that CO_2 bound to an amine could be electrochemically converted to CO with an FE of 72% at 50 mA/cm^2. These integrated CO_2 capture and conversion methods are promising, but more research and optimization is required to assess their potential for scale-up.

As a possible solution, a two-step process has been proposed to overcome the limitations posed by the direct electrochemical reduction of CO_2 in alkaline media.[16−18] In the first step, CO_2 is converted to CO in neutral to slightly acidic conditions to prevent bicarbonate formation. In a subsequent step, CO is electrochemically reduced (COR) in alkaline media to desired C_{2+} products such as ethylene. The advantage of the two-step process is that (1) the parasitic loss of CO_2 and bicarbonate precipitation in the GDE are avoided, because CO does not react with the electrolyte; (2) the FEs for C_{2+} products in the second step are higher, because COR requires fewer electrons than CO2R; and (3) higher reaction rates and reactant conversion are observed for COR. Furthermore, it is important to note that (1) the product distribution of COR can be different than that for CO2R, (2) COR in alkaline media also results in the dissociation of carboxylic acids to carboxylates (e.g., acetate), and (3) CO can react with water, nonaqueous solvents, and alkaline electrolytes, but typically high temperature and pressure conditions are required. In the worst case, the two-step conversion will require two electrolyzers, which will significantly affect the capital cost of the process. In the best case, the two electrolyzers can be integrated into a single electrolyzer stacked alternately with two different types of catalyst.[19] For example, by using silver catalysts in the first stack CO_2 can be converted to CO, which is further reduced in a second stack of copper-based catalysts to C_{2+} products. The concept of such an integrated electrolyzer is interesting, but might be difficult to implement in practice due to the increased complexity of the process, which requires management of different reaction conditions (pH, temperature, pressure), product and recycle streams, and lifetime of catalysts. However, the increased CAPEX of the two-step process, whether integrated into a single electrolyzer or not, relative to the direct CO2R process might be offset by the higher FEs, CDs, single-pass conversion, and CO_2 utilization (i.e., lower OPEX). Therefore, the choice between direct CO2R and the two-step CO2R/COR conversion to C_{2+} products will be governed by the economics and scalability of both processes. Several studies reported the techno-economics of CO_2 reduction to ethylene, but none of these considered a realistic downstream processing of the CO2R or COR to C_2 products.[20−28]

Here, we will perform a detailed process design and techno-economic analysis of the direct CO2R process and the two-step conversion of CO_2/CO to C_2 products including ethylene, ethanol, and acetic acid. The design and economic analysis include CO_2 capture, electrochemical CO_2 and CO conversion, reactant recycling, and downstream product separation. An extensive literature review is performed, and the currently best available technologies (BATs) for CO_2 separation, electrochemical CO_2/CO conversion, and product separation are selected for the process design. It is very unlikely that CO_2 or CO electrolyzers will operate on a standalone basis due to the requirement of different feedstocks and the challenges related to the condensation, storage, transportation, and distribution of a range of difficult to handle products. Therefore, to improve the economics, we investigate different strategies to integrate the CO_2/CO electrolyzer into the existing chemical industry infrastructure. The best integration options are selected on the basis of the product distribution and process conditions for CO2R and COR. We present guidelines for the design, scale-up, integration, and implementation of CO_2/CO electrolyzers on industrial relevant scales.

In the following, we will start with a literature review of technologies and methods for the different processing steps in the value chain. On the basis of this review, the best available technologies/methods will be selected for the process design modeling in the next section. Aspen Plus will be used for detailed flowsheeting, optimization, and sizing of process units, and to estimate capital and operating costs of the downstream process. In a subsequent section, an economic analysis of the full value chain for producing chemicals from CO_2 will be presented. Next, strategies for integrating the CO_2 electrolysis process into the existing infrastructure are outlined. In a follow-up section, the main barriers that impede successful implementation of CO_2 electrolyzers on a commercial scale are discussed. Finally, we will summarize the outcome of this study and present the main conclusions.

STATE OF THE ART OF CO2R AND COR TO C_{2+} PRODUCTS

The research on CO2R and COR to hydrocarbons started in the 1980s with the pioneering work of Hori.[29,30] At that time, both reactions were performed in the liquid phase, which caused significant mass transfer limitations due to the poor solubility of CO_2 and CO in aqueous electrolytes. It is now

https://doi.org/10.1021/acs.iecr.1c03592
Ind. Eng. Chem. Res. XXXX, XXX, XXX−XXX

generally recognized that gas diffusion electrodes are indispensable for CO2R or COR at industrial scale current densities. So far, only copper-based catalysts with varying morphologies have been demonstrated to reduce CO_2 or CO with a reasonable selectivity and reaction rates to C_{2+} products. In Table S1, we have compiled a list of landmark studies that reported current densities higher than 100 mA/cm^2 for CO2R to C_{2+} products.[31−44] In Table S2, a compilation of interesting studies on CO reduction to C_{2+} products is provided.[45−54] We note that several studies reported high FEs for C_{2+} products but at much lower CDs, which is less interesting from an economic point of view and have been excluded from the list. As noted by Romero Cuellar et al.[45] and Xia et al.,[55] COR has a few advantages compared to CO2R: (1) the FEs for C_{2+} products are higher, because COR typically requires a lower number of electrons for a specific product; (2) the current densities are higher due to the higher reactivity of CO, which results in a higher single-pass conversion of CO; (3) the cell potential is lower for COR and (4) the CO_2 utilization efficiency is higher for COR because of the parasitic loss of CO_2 in CO2R due to reactions with the electrolyte. Furthermore, it is clear that the main CO_2/CO electroreduction products on copper-based catalysts are ethylene, acetic acid/acetate, ethanol, propanol, and hydrogen. All three liquid products (i.e., acetic acid, ethanol, and propanol) exhibit an azeotropic behavior with water, which will add significant expenses in the downstream process. Strictly speaking, the acetic acid/water system shows a pinch point, which is like an azeotropic point difficult/impossible to overcome by ordinary distillation. Therefore, in practice, azeotropic distillation is used to obtain pure acetic acid. It is important to note that the reaction pathway can be steered to some extent to yield higher fractions for one of these products by controlling the composition, size, morphology, grain boundaries, oxidation states, type of dopants, facets, fragmentation, dealloying, confinement, and porosity of the catalyst.[56−59] Even cofeeding of CO_2/CO mixtures on Cu catalysts seems to have a significant effect on the product distribution.[60] Many of these selectivity controlling measures (especially morphologies, facets, and grain boundaries) are affected at high current densities and results in performance degradation over time. However, the key characteristic of CO2R or COR on copper catalysts is that a multicomponent mixture is obtained as product, which requires purification to meet customer specifications.

Furthermore, a very concerning experimental observation is that for C_{2+} products a relatively pure CO_2 or CO stream is required. A dilute CO_2 stream results in a low CO_2 coverage of the catalyst surface, which affects the C−C coupling process and shifts the mechanism from C_{2+} products to methane.[61] The main consequence of this observation is that typical industrial CO_2 or CO streams cannot directly be used in the electrochemical process, but will require a purification step to increase the concentration. Therefore, upstream and downstream separation, and smart system integration, will play a crucial role in reducing the cost of CO_2 electroreduction products. Recently, a tandem catalysis approach has been used to demonstrate efficient CO_2/CO electroreduction to C_{2+} products for some specific CO_2/CO ratios.[60] In this case, a separation step will also be required, because industrial CO_2/CO streams often contain nitrogen, methane, hydrogen, and other impurities. We note that neither the liquid products nor the involved gas mixtures from a CO_2/CO electrolyzer are easy to separate. CO_2 forms an azeotrope with ethylene, which means that cryogenic distillation cannot be used for product purification. Similarly, the separation of CO from ethylene is also not straightforward due to their similar kinetic diameters and adsorption behavior. In Process Design and Modeling, we will present some guidelines to separate such a multicomponent mixture, which is not a trivial task due to the presence of several gases, liquids, recycle streams, and azeotropes.

In the two-step process, CO_2 is first converted to CO, which is further reduced in a subsequent step to C_{2+} products. For this reason, in Table S3, we have compiled a list of groundbreaking studies on CO_2 reduction to CO.[11,62−79] The main goal of the two-step process is to minimize the loss of CO_2 due to (bi)carbonate formation, which can only be achieved when the reaction is performed in acidic or neutral conditions. However, most of the studies were performed in alkaline conditions, but it is possible to obtain relatively high FEs for CO in slightly acidic or near-neutral conditions and in membrane electrode assembly (MEA) based cells.[79−81] An alternative technology, based on a solid oxide electrochemical cell (SOEC), has been developed and commercialized by Haldor Topsoe to convert CO_2 to CO, which has a claimed energy requirement of 6−8 kWh/Nm^3 CO.[82] Furthermore, many industrial (purge) streams already contain substantial amounts of CO, which can be utilized (after purification) in the second step of the process. Note that it is crucial to have a high conversion of CO_2 in the first step. Otherwise, a mixture of CO_2 and CO is obtained, which will cause CO_2 loss in the second step and compromise the benefits of the two-step process. Often, the FE is not 100% and a mixture of CO and hydrogen (i.e., syngas) in a variety of ratios is produced. If both the conversion and FE are <100%, then a mixture containing CO_2, CO, and hydrogen is obtained. In the second step, which is performed in alkaline conditions, part of the CO_2 will be converted to bicarbonates, while the presence of hydrogen might result in the hydrogenation of ethylene. An option is to purify the reaction mixture from the first step before feeding to the second step, but this will increase the costs of the two-step process.

It is clear from the foregoing discussion that both processes, i.e., the direct CO2R process and the two-step CO2R/COR process, need to be designed carefully for optimal functioning. In Process Design and Modeling, we will present a detailed process modeling of both processes, including CO_2 capture, CO_2 conversion, reactant recycling, and downstream separation of products. A detailed discussion on downstream separation is presented with the aim to help electrochemists in making catalyst and process design decisions. For this reason, a relatively complex (gaseous and liquid) mixture is chosen for the downstream separation.

PROCESS DESIGN AND MODELING

In this section, we will present the process design and modeling of the direct CO2R to ethylene (i.e., the single-step process) and the indirect CO2R/COR to ethylene (i.e., the two-step process). The modeling of both processes includes CO_2 capture from a point source, electrochemical conversion of CO_2, recycling of reactants, and downstream separation of the multicomponent product mixture. As we will show later, it is better to integrate the CO_2 electrolysis process into the existing (oil and gas) infrastructure to minimize costs for purification, transportation, storage, and distribution of

https://doi.org/10.1021/acs.iecr.1c03592
Ind. Eng. Chem. Res. XXXX, XXX, XXX−XXX

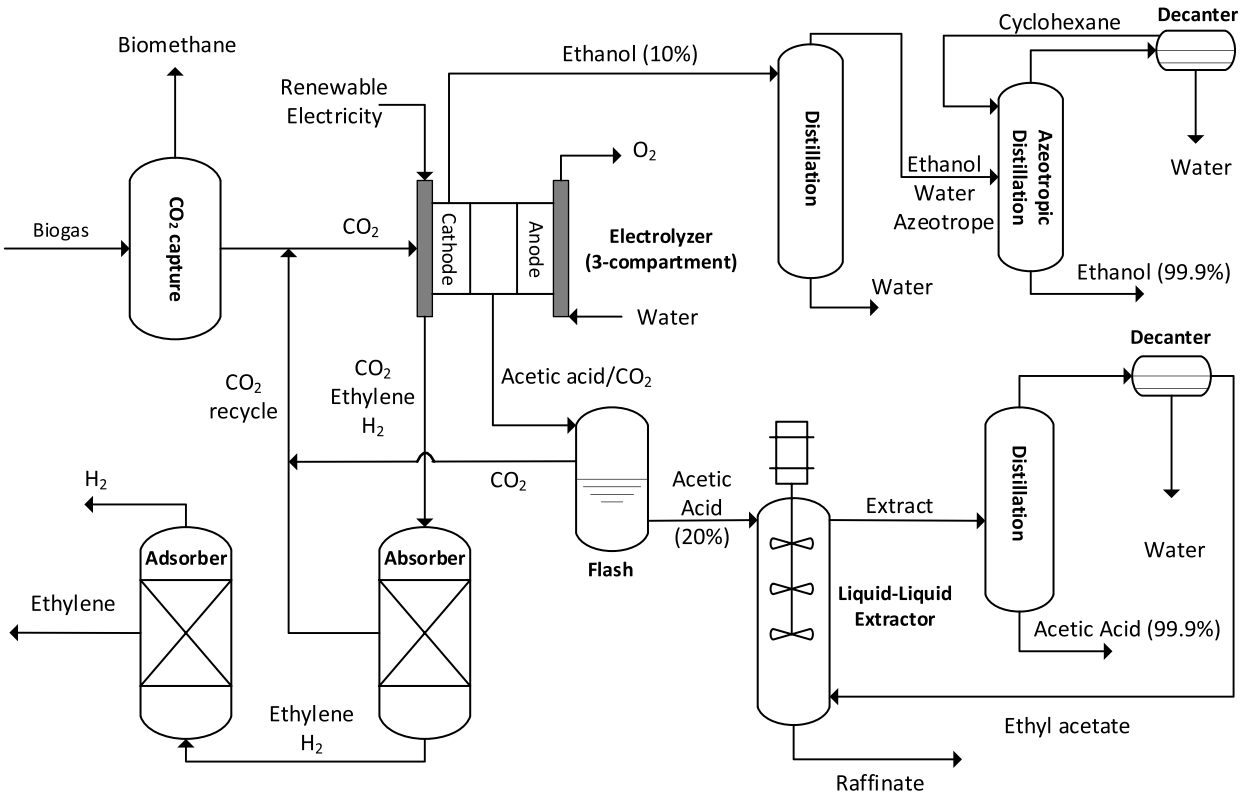

Figure 1. Overview of the single-step process for CO2R to C_2 products. CO_2 is captured from biogas (40% CO_2 and 60% methane) and fed to the electrolyzer, which converts CO_2 to ethylene, ethanol, and acetate. The electrolyzer is operated in alkaline conditions in a three-compartment configuration, which converts the acetate to acetic acid in the center compartment. An amine absorber is used to separate the unconverted CO_2, which is recycled back to the electrolyzer. The remaining ethylene/H_2 mixture is separated in an adsorber using activated carbon. The acetic acid stream from the center compartment is flashed to separate dissolved CO_2, which is recycled to the electrolyzer. The liquid stream from the flash is fed to the liquid−liquid extractor, which uses ethyl acetate to extract acetic acid. The extract is sent to the azeotropic distillation column, where pure acetic acid is obtained as bottoms, while an azeotropic mixture of water and ethyl acetate is distilled and condensed in two liquid phases in a decanter. The ethyl acetate rich stream from the decanter can be recycled to the extractor. The water-rich stream from the decanter and the raffinate stream from the extractor are typically combined and sent to the water treatment (not shown). The ethanol stream from the cathode compartment is sent to an ordinary distillation column, which can purify ethanol up to the azeotropic point. This ethanol stream is dehydrated in an azeotropic distillation column using cyclohexane as entrainer. Almost pure ethanol is obtained in the bottom of the azeotropic distillation column. The distillate, which is a ternary azeotropic mixture, is sent to a decanter to condense two liquid phases. The cyclohexane-rich phase is recycled to the azeotropic distillation column, while the water-rich phase is sent to a stripper (not shown).

reactants and products. However, here we will design an autonomous decentralized power-to-ethylene process, which excludes any integration. This is done on purpose to have a system independent benchmark case and to demonstrate the importance of process integration. For the single-step CO2R to ethylene process, only low temperature (<100 °C) electrolysis will be considered, since high temperature electrolysis of CO_2 has only been demonstrated for CO or syngas as the main products. For the two-step CO2R/COR process, low and high temperature electrolysis (e.g., the solid oxide electrochemical process of Haldor Topsoe) will be considered.

We will design a process that can convert 10 ton/h CO_2 to C_{2+} products with the assumption that only ethylene, ethanol, and acetic acid are formed in the CO2R and COR processes. In addition, we assume that hydrogen is the only gaseous byproduct that is formed in both processes. These compounds typically account for the majority of the C_2 products (>90%), with the remainder being a mix of C_1 and C_3 products. We implicitly assume that with proper catalyst and process design the formation of C_1 and C_3 products can be suppressed. If the development of such a selective catalyst remains elusive, much more complicated downstream processing will be required than presented here. We assume that the COR process has a slightly higher conversion than CO2R (75% vs 50%), which can be justified on the basis of recent experimental results. The CO_2/CO electrolyzers will be operated at elevated pressures (10 bar) to achieve a higher single pass conversion. We assume that the concentrations of ethanol and acetic acid are 10 and 20% (w/w), respectively. These numbers depend on the reaction conditions (e.g., flow rate of reactants and catholyte, FE, and conversion), which cannot be changed independently in a real process. The concentration of ethylene cannot be chosen independently if the conversion is fixed, but the concentration of liquid products can be varied by changing the supply rate of water to the cathode or center compartment of a three-compartment cell. In the Supporting Information (section S6), we have calculated the concentrations of ethanol and acetic acid as a function of the water supply rate for different cell configurations (zero-gap and flow cells). It is important to note that much higher ethanol concentrations will likely require new membranes, because Nafion membranes can only tolerate small amounts of organics (<10 wt %). The concentration of acetic acid is based on the current status of electrochemical CO_2 conversion to formic acid, which

https://doi.org/10.1021/acs.iecr.1c03592
Ind. Eng. Chem. Res. XXXX, XXX, XXX−XXX

produces around 20 wt % formic acid. In the following, a detailed process modeling of both processes is presented.

Process Design for CO2R to C_2 Products. An overview of the CO_2 to ethylene process is provided in Figure 1. We capture CO_2 from a relatively high partial pressure stream (e.g., biogas) using absorption with amines. The costs of CO_2 capture from biogas using membranes, pressure swing adsorption (PSA), and scrubbers are very similar for large scale processes and are in the range \$25−50/ton CO_2.[7] The cost of CO_2 capture from air is a factor of 5−10 higher and will not be considered here.[83] The captured CO_2 is fed to a high pressure (10 bar) GDE-based electrolyzer, which converts CO_2 to ethylene, acetate, and ethanol. Note that the CO_2 feed to the electrolyzer does not necessarily need additional pressurization, because CO_2 from a biogas plant is often available at elevated pressures. The electrolyzer is operated in alkaline media using a three-compartment configuration, which converts acetate to acetic acid in the center compartment. For the base case of the CO2R process, it is assumed that ethylene, ethanol, acetic acid, and hydrogen are produced at a total CD of 500 mA/cm^2 with FEs of 50, 20, 20, and 10%, respectively. It is difficult to choose a distribution for the products, since it depends on many factors such as temperature, pressure, catalyst type and morphology, cell potential, current density, pH, and type of reactant (CO_2/CO). We have fixed the Faraday efficiency of ethylene and that of hydrogen to 50 and 10%, respectively, which is realistic as can be seen in Tables S1 and S2. The Faraday efficiencies of ethanol and acetic acid are highly condition dependent, but CO2R tends to produce more ethanol than acetic acid while this seems to be the opposite for COR. For simplicity, we have decided to use an FE of 20% for both components. Later, we will show that the distribution of the C_2 products does not matter much for the economics.

At the assumed conditions and a CO_2 conversion of 50%, the outlet concentrations of ethylene, CO_2, and hydrogen are 16, 65, and 19 mol %, respectively. The gaseous ethylene, hydrogen, and unconverted CO_2, and the liquid containing around 10 wt % ethanol from the cathode compartment are separated in a flash tank. The gas stream from the flash mostly contains ethylene, hydrogen, and CO_2, which is sent to the gas purification section (GPS). The aim of the GPS is to provide a nearly pure ethylene stream, recycle the unconverted CO_2, and recover as much as possible hydrogen with a high purity. Such a separation cannot be achieved in a single unit but will require multiple (at least two) steps to obtain the desired products. The technologies available for separating hydrogen/CO_2/ethylene mixtures include absorption, adsorption, membranes, and cryogenic distillation. By using an elimination procedure, one can select the most suited technology for the separation. The starting point is that CO_2/ethylene selectivities of existing membranes and adsorbents are relatively low. Several recent techno-economic studies have used pressure swing adsorption to separate CO_2/ethylene mixtures without specifying the adsorbent.[20,22,27,84] To the best of our knowledge, currently available industrial adsorbents cannot be used for efficient CO_2/ethylene separation due to their similar adsorption behaviors. In principle, hydrogen selective membranes and adsorbents could be used, but these processes typically require much higher hydrogen concentrations (>40 mol %) to justify the economics. Cryogenic distillation cannot be used, because CO_2 and ethylene form an azeotrope and CO_2 will cause dry ice formation in the column.[85] From this elimination procedure, absorption appears to be the most interesting option for the first separation step.

In the absorber, a physical solvent (e.g., Selexol) could be used to remove CO_2, because the partial pressure of CO_2 is relatively high (∼6.5 bar). However, the CO_2/ethylene selectivity of classical solvents (e.g., Selexol, NMP, Purisol, and Rectisol) is very low (around 2−3),[86] which will result in a high ethylene concentration in the CO_2 recycle stream. In principle, the ethylene in the recycle is not lost but will dilute the CO_2 feed to the electrolyzer, which might affect the CO2R process. The CO_2/ethylene selectivity in water is around 10,[87] but the feed stream needs to be pressurized, because the solubility of CO_2 in water is relatively low. For this reason, we have decided to use a chemical solvent (e.g., a monoethanolamine (MEA) solution) to selectively remove CO_2 from the ethylene and hydrogen mixture. The absorption of CO_2 is performed at the high feed pressure (∼10 bar), which is not necessary for chemical solvents but is beneficial as repressurization of the ethylene/hydrogen stream is avoided. On the other hand, the CO_2 recycle stream needs to be pressurized, because the CO_2 desorption step is performed at low pressures. The gas stream after the CO_2 capture step will likely be saturated with water, which is not desired for downstream processes (e.g., membranes, adsorbents, and ethylene reactions). In the process design and economics, the drying step to remove water is neglected. After removal of all the CO_2, the concentrations of ethylene and hydrogen are increased from 16 to 45 mol % and from 19 to 55 mol %, respectively. Such a mixture is often present in industrial streams (e.g., ethylene off-gas or refinery off-gas) and can be separated by membranes, PSA, or cryogenic distillation. The selection between these technologies depends on the operating conditions and requirements (feed pressure, feed composition, flow rate, desired purity, (by)product recovery, process flexibility, turndown ratio, reliability, and scale-up considerations). Guidelines for selecting a hydrogen separation process are provided by Benson et al.[88] and Miller et al.[89] We have considered membranes and adsorption to separate hydrogen from ethylene. Note that for membranes ethylene will be obtained approximately at feed pressure, since hydrogen will selectively permeate through the membrane. For adsorption, hydrogen will be obtained at feed pressures, since ethylene is selectively adsorbed on the adsorbent. This means that, in the case of membranes, the hydrogen stream needs to be compressed for storage or transportation, but at low pressures it could be used on-site as fuel. We have neglected these details in the process design, but they are important to consider in a real process. The selectivity and permeability data of hydrogen and ethylene in polyamide membranes of UBE were taken from Al-Rabiah et al.[90]

The countercurrent hollow fiber membrane model of Pettersen and Lien[91] was used for the design calculations. In this algebraic model, the permeate mole fraction of component i is calculated from known feed concentrations and design variables such as the molar stage cut, pressure ratio, and a dimensionless permeation factor, which is related to the membrane area. The simplified model of Pettersen and Lien[91] is suitable for multicomponent mixtures and can easily be implemented in flow sheet calculations. In the Supporting Information (section S2), we show that it is hard to achieve 99% purity for ethylene using commercial membranes. A purity of 85−90% can be achieved with a single-stage membrane process using a stage cut of around 0.5 and a pressure ratio of

https://doi.org/10.1021/acs.iecr.1c03592
Ind. Eng. Chem. Res. XXXX, XXX, XXX−XXX

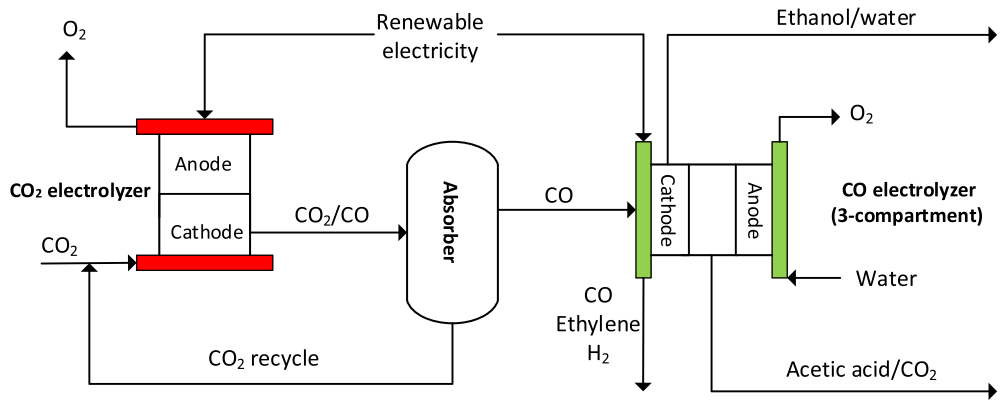

Figure 2. Two-step (tandem) CO_2/CO electrolysis to value-added products. CO_2 is first converted to CO in a high temperature (e.g., SOEC) or low temperature CO_2 electrolyzer. The unconverted CO_2 is removed from the product mixture using an amine absorber. The nearly pure CO is converted to ethylene, ethanol, and acetic acid in a CO electrolyzer operated in a three-compartment configuration. The downstream separation of the gases and liquids is similar to the single-step CO2R process. More details are provided in the text.

10. The purity can be increased by using a cascade of membranes, but this will significantly increase the separation costs. Therefore, we have decided to use adsorption for the separation of ethylene from hydrogen with activated carbon as adsorbent. A five-bed vacuum pressure swing adsorption (VPSA) process was designed to recover ethylene with a purity of >99%. The adsorption process was modeled at 25 °C and 10 bar feed pressure. No feed pressurization was required, since the pressure at the electrolyzer outlet is 10 bar. VPSA processes include the following four basic steps: (1) adsorption, where the feed enters the bed at the bottom and nonadsorbed components leave at the top; (2) blow down, where the bed is partly regenerated by releasing the pressure to the atmosphere; (3) evacuation, where the bed pressure is reduced further with a vacuum pump to achieve higher regeneration levels; (4) and repressurization, where the bed pressure is increased to a level similar to that in the adsorption step. Often, one or more of these basic steps are included to increase the performance of the process (i.e., increase the purity and/or recovery, decrease the energy costs, etc.). In our process, three pressure equalization steps were used for the separation of H_2 and ethylene. More details of the VPSA process can be found in the Supporting Information (section S3). The purities of ethylene and hydrogen were 99.5 and 97.5% at recoveries of 97 and 99%, respectively. Note that the purity specifications for ethylene depend on the application. For example, for polymerization processes at least 99.9% ethylene is required, while other processes (e.g., vinyl acetate) can tolerate higher concentrations of impurities. Therefore, the ethylene stream from the adsorption unit might require some polishing steps to remove traces of H_2 and other impurities. These polishing steps are not included in the process design and techno-economic evaluation.

The acetic acid stream from the center compartment is flashed to separate CO_2, which results from the protonation of bicarbonate. Due to the operation in alkaline media, (bi)carbonate is formed and transported through the anion exchange membrane to react with the protons from the anode to give water and CO_2 in the center compartment. We have assumed that all hydroxide ions generated in the CO2R process will be converted to (bi)carbonate; see the Supporting Information (section S7) for more details. The liquid stream from the flash contains around 20% acetic acid, which is further purified in a hybrid liquid−liquid extraction followed by an azeotropic distillation process. It is well-known that liquid−liquid extraction is the most economic method to separate acetic acid from dilute streams (i.e., concentrations of <30%).[92] We have used ethyl acetate as the extracting solvent, which is the industrial standard for acetic acid separation. The extract containing acetic acid, ethyl acetate, and coextracted water is fed to the azeotropic distillation column. In this column, an azeotropic mixture of water and ethyl acetate is obtained as distillate, while almost pure acetic acid is obtained as bottoms. Water and ethyl acetate form a heterogeneous low boiling azeotrope, which can be separated in a decanter into an ethyl acetate rich stream (which is recycled to the extraction column) and a water-rich stream, which is sent to the raffinate treatment process (not shown). The liquid−liquid extraction process was designed and modeled in Aspen Plus according to the procedures outlined by Shah et al.[93] The extractor was modeled with the EXTRACT unit block in Aspen Plus and operated at 25 °C and 1 bar. The number of stages and the solvent flow in the extractor were optimized for an acetic acid recovery of 99.0 wt %. The optimization was performed with the constraint that the extraction factor should be between 1.5 and 2. For the design, the number of stages was set to 15 and a solvent flow of 25 000 kg/h was chosen. For more details on the liquid−liquid extraction process, the reader is referred to the Supporting Information (section S5).

The ethanol stream from the flash tank can be purified further in an ordinary distillation column up to the azeotropic point (95.6 wt % ethanol). If anhydrous ethanol is desired, an additional step will be required to break the low boiling azeotrope by, for example, azeotropic distillation, extractive distillation, membranes, or adsorption. We will concentrate the ethanol stream up to 99.9% using azeotropic distillation with cyclohexane as the entrainer. The distillation column was modeled in Aspen Plus using the RADFRAC unit block. The distillation columns were optimized using two design specifications: (1) the purity of the ethanol stream and (2) the ethanol mass recovery. The reflux ratio and the bottoms rate were varied to meet the design specifications. The Model Analysis tool in Aspen Plus was used to optimize the number of stages and the feed stage by reducing the reboiler duty. See the Supporting Information (section S4) for the optimized parameters of the distillation column.

The proposed process in Figure 1 was simulated, from which the capital and operating costs of all the units (electrolyzers,

https://doi.org/10.1021/acs.iecr.1c03592
Ind. Eng. Chem. Res. XXXX, XXX, XXX−XXX

absorbers/adsorbers, membranes, extraction and distillation columns) were derived. More details are provided under Economic Analysis of Value Chain.

Process Design for CO2R/COR to C_2 Products. The design of the two-step (CO2R/COR) process is very similar to the single-step CO2R process explained in the previous section. The only difference is that the CO_2 electrolyzer in the single-step process is replaced by a couple of CO_2 and CO electrolyzers in the two-step process, as shown in Figure 2. In the first electrolyzer, CO_2 is converted to CO, which is further reduced in the second electrolyzer to C_2 products. Two cases are considered for the conversion of CO_2 to CO: (1) low temperature electrolysis and (2) high temperature electrolysis using a SOEC. Recently, Küngas et al.[94] reviewed the advantages and disadvantages of both technologies. The high temperature SOEC process for CO production has a few advantages over the low temperature process; i.e., the electric power consumption of the SOEC is much lower, the Faraday efficiency is higher (near 100%), the conversion of CO_2 to CO is higher, the stability of the cell is higher and the degradation rate is lower, the overpotentials are lower, and the technology readinesss level (TRL) is higher (SOEC is nearly commercial). It is important to note that the conversion of CO_2 in both (high and low temperature) processes is less than 100%, which means that a mixture of CO and unconverted CO_2 will be obtained as product in the first electrolyzer. In the low temperature process, the first electrolyzer is operated at high pressures but in nonalkaline conditions to minimize the loss of CO_2 due to bicarbonate formation. In the first electrolyzer, we assume Faraday efficiencies of 95% for CO and 5% for hydrogen at a current density of 300 mA/cm^2 and a cell voltage of 2.5 V. Furthermore, we assume a CO_2 conversion of 50%.[95] The small amount of hydrogen is neglected in the process design (i.e., no downstream processing is designed for the separation of hydrogen from CO and unconverted CO_2). The CO_2/CO mixture from the first electrolyzer can in principle directly be fed to the second electrolyzer, but initial experimental results show that the presence of large amounts of CO_2 in the mixture has a detrimental effect on the product distribution.[46]

Since the second electrolyzer is operated in alkaline conditions, part of the CO_2 from the outlet of the first electrolyzer would be converted to (bi)carbonate, compromising the usefulness of the two-step process. Therefore, in the process design, we have decided to separate the CO_2 from the CO_2/CO mixture using amines. The captured CO_2 is recycled to the first electrolyzer, while the almost pure CO is fed to the second electrolyzer, which is operated at high pressure (10 bar) in a three-compartment configuration. We again assume that only ethylene, ethanol, acetic acid, and hydrogen are produced in the second electrolyzer. As explained earlier, the FE, CD, concentration, and conversion of the COR process is slightly higher than that of the single-step CO2R process. For the base case of the COR process, we have assumed that ethylene, ethanol, acetic acid, and hydrogen are produced at a total CD of 750 mA/cm^2 with FEs of 50, 20, and 20, and 10%, respectively. Clearly, the partial CD of the products in the COR process is assumed to be higher than that in the CO2R process. At these conditions and a conversion of 75%, the outlet concentrations of ethylene, CO, and hydrogen are 31, 45, and 24 mol %, respectively. Furthermore, the concentrations of ethanol and acetic acid are 10 and 20% (w/w), respectively. The concentrations of ethanol and acetic acid are kept the same as in the CO2R process to reduce the (possibly dominating) effect of the liquid separations on the overall cost. Note that the concentration of acetic acid can be controlled independently by the flow rate of water in the center compartment. The concentration of ethanol depends on the water supply rate at the cathode.

The purification steps for acetic acid and ethanol are the same as in the single-step process. The separation of ethylene from CO/H_2 is far more challenging than that from CO_2/H_2. The reason for this is that CO and ethylene have very similar kinetic diameters, diffusion properties, and adsorption behaviors. Methods for CO separation, but not necessarily in the presence of ethylene, can be found in the paper of Dutta and Patil.[96] Commercial membranes are not suitable for the separation of CO and ethylene mixtures, because the CO/ethylene selectivity is very low. Cryogenic separation is not selected due to the high operating costs. Since the pressure is relatively high, physical solvents such as Selexol and NMP, which show relatively high ethylene solubilities and ethylene/CO selectivities (~10), could be used. We will use adsorption to separate ethylene from a CO/H_2 mixture. Many different types of adsorbents have been reported for ethylene/ethane separation, but adsorption studies on CO/ethylene separation are scarce. Bachman et al.[97] studied the adsorption of ethylene from different gases including CO using metal−organic frameworks (MOFs) and a commercial zeolite CaX, which exhibited a relatively high ethylene/CO selectivity. However, these adsorbents are expensive, in particular the MOFs, which also have some stability issues in the presence of water. We have selected activated carbon for the separation of ethylene from the CO/H_2 mixture. A five-bed VPSA process was designed to recover ethylene with a purity of at least 99%. The adsorption process was modeled at 25 °C and 10 bar feed pressure. The basic steps in the VPSA cycle are similar to the one discussed for H_2/ethylene separation in the previous section. Here, we have used two pressure equalization steps and a purge step to purify the ethylene stream. In the purge step, partial ethylene product is pumped back into the adsorption bed from the bottom before the blow down step moving impurities up from adsorbents or void spaces for obtaining a clean product in the following desorption step. The purge gas amount is 63% of total ethylene desorption gas amount. Note that in this case an additional compressor is needed to pump ethylene from 1 bar (after vacuum pump) to 10 bar for purging the bed. The technical details of the VPSA process can be found in the Supporting Information (section S3). The five-bed VPSA system is able to recover 76% of the ethylene with a purity of 99% (the remaining 1% is mainly CO). It is not possible to obtain higher recoveries with the current VPSA process with activated carbon as adsorbent. Therefore, it is highly desired to develop better adsorbents for CO/ethylene separation. The syngas-rich stream leaving the adsorber contains around 10% ethylene, 31% hydrogen, and 59% CO. This ethylene containing syngas mixture can be utilized on-site as a fuel, but it is better to recover the hydrogen and to recycle the valuable reactant (CO) and product (C_2H_4) to the electrolyzer. We have separated the C_2H_4/CO/H_2 mixture with a polyimide membrane into a CO-rich stream (including ethylene), which is recycled to the electrolyzer, and a H_2-rich stream, which can be used as fuel or purified further for storage and transportation. The model of Pettersen and Lien[91] and the C_2H_4/CO/H_2 permeability/selectivity data from Al-Rabiah et al.[90] were used to design the membrane

https://doi.org/10.1021/acs.iecr.1c03592
Ind. Eng. Chem. Res. XXXX, XXX, XXX−XXX

process. The details of these calculations can be found in the Supporting Information (section S2).

In the high temperature SOEC process, CO_2 is electrochemically converted at 700−850 °C to CO. In the absence of water in the feed, the SOEC process does not produce hydrogen as a byproduct. For the SOEC, we do not assume Faraday efficiencies, current densities, and cell voltages, but we compute the required power to convert 10 tons/h of CO_2 directly from the energy consumption reported by Haldor Topsoe (6 kWh/Nm^3 CO).[82] A high degree of conversion is avoided in the SOEC process to limit carbon formation from the Boudouard reaction. The concentration of CO at the exit of the SOEC is typically between 20 and 80 wt %, which corresponds to conversions of approximately 30 and 85%, respectively. In the Haldor Topsoe process, the CO_2 is captured from the CO_2/CO mixture using PSA and recycled back to the SOEC. In the process design, we will assume a CO_2 to CO conversion of 75%, which is higher than that of the low temperature CO2R process. As mentioned earlier, a mix of CO_2 and CO has a possibly negative effect on the product distribution, FEs of C_2 products, and CO_2 utilization efficiency. For this reason, the CO_2/CO mixture from the SOEC will be purified before feeding to the COR process. We have used absorption with amines to remove the CO_2 from the CO_2/CO mixture, because the CO_2 partial pressure is relatively low as the SOEC is operated at atmospheric pressures. The captured CO_2 is recycled back to the SOEC, while the pure CO is reduced in the second (low temperature) electrolyzer to C_2 products. This electrolyzer is operated at high pressure and alkaline conditions in a three-compartment configuration. The remaining steps and assumptions are the same as in the low temperature electrolysis process. An advantage of the high temperature SOEC process is that the excess heat can be integrated with the ethanol and/or acetic acid distillation columns.

■ ECONOMIC ANALYSIS OF VALUE CHAIN

To assess the potential of CO2R and COR to ethylene, a detailed economic analysis of the full value chain, including CO_2 capture, electrochemical conversion, reactant recycling, and product separation has been performed. Two cases have been considered for the conversion of CO_2 to ethylene. In the first case, CO_2 is directly converted to ethylene in alkaline media (i.e., the single-step process). In the second case, CO_2 is first converted in acidic or neutral conditions to CO, which is subsequently converted to ethylene (i.e., the two-step (tandem) process). The estimation of the capital and operating costs of all components in the value chain involve some degree of uncertainty. To take this variability into account, a sensitivity analysis will be performed to investigate the effects of different parameters on the process economics. For the base case, we will use the currently best available estimates for the cost components. In case of lacking data, we will estimate the costs based on closely related processes (e.g., water electrolysis). The base case will be supplemented with two additional (worst and best case) scenarios. In the following, we will shortly discuss some of the parameters (CO_2 price, electricity price, CAPEX and OPEX of CO_2 electrolyzers, and product selling price) that significantly effect the cost analysis.

Base Case Assumptions. For the price of CO_2, we have used the Sherwood (cost versus concentration) correlation of Bains et al.:[98]

$$\log_{10}[\text{cost}/(\$/\text{kg})] = -0.5558 \log_{10}[\text{mole fraction of } CO_2] - 1.8462 \quad (2)$$

This correlation is based on cost data for different gas capture technologies (NO_x, SO_x, and CO_2) calculated with the Integrated Environmental Control Model (IECM) by Rubin. The correlation of Bains et al.[98] accounts for CO_2 capture costs including CAPEX and OPEX, but it excludes costs related to compression, transportation, and storage. To decouple the CAPEX and OPEX costs, we have assumed a CAPEX to OPEX ratio of 25% to 75% (i.e., 25% of the cost ($/kg) is due to CAPEX and 75% is due to OPEX). The cost of CO_2 capture can be calculated once the CO_2 concentration in the feed is known (the higher the concentration the lower the capture cost). For CO_2 capture from flue gas with 10% CO_2, the correlation predicts a cost of around $50/ton, which is in good agreement with costs reported for commercial scale processes (e.g., Boundary Dam and Petra Nova[99]). In our process design, CO_2 is captured from a biogas plant with a concentration of 40% CO_2, which results in a CO_2 capture cost of ∼$25/ton. The concentration of CO_2 in the product mixture, hence the cost of recycling, depends on the conversion in the electrolyzer. We assumed that all CO_2 reacted to (bi)carbonate is recovered in the three-compartment cell and recycled to the process. Finally, we note that the effects of carbon taxes or credits, and other climate change policies on the CO_2 price, were not considered in the techno-economic analysis.

The electricity price has a huge influence on the cost of power-to-X processes, including CO_2 electrolysis to chemicals and fuels. It is crucial to use electricity from renewable energy sources to have a significant impact on the CO_2 emissions. Using electricity generated from an energy mix with a high carbon intensity will compromise the usefulness of power-to-X concepts. Before the COVID-19 pandemic, the wholesale prices of electricity in Europe were between $40/MWh and $50/MWh, which decreased to $20/MWh just after the COVID-19 outbreak, but the prices are now bouncing back to the old level.[100] For most European countries the share of renewable energy is still relatively low, but it is expected to increase rapidly. However, the cost of electricity (COE) in countries that do have a high share of renewables in the energy mix (e.g., Scandinavian countries) is similar to the COE in countries with a low degree of renewable energy sources. A few conclusions can be derived from this observation: (1) renewable energy sources such as solar and wind are already competitive with conventional (fossil-based) electricity generation technologies; (2) the high share of renewables does not necessarily lead to lower electricity prices, because the cost is also determined by other factors (e.g., taxes and levies, market competition, environmental policies and regulation, supply and demand, etc.); and (3) in the short term it will be very challenging to have an electricity price lower than $20/MWh. Recently, the U.S. Energy Information Administration (EIA)[101] and Lazard[102] estimated the levelized cost of electricity (LCOE) from renewable sources (wind and solar) to be around $30/MWh. It is important to realize that electricity prices have a huge impact on the economics of power-to-X concepts, because the operating cost is typically dominant. In the techno-economic analysis, we do not consider operating the process in an intermittent mode (e.g., running the process only during off-peak hours when the electricity price is low or negative). It is very unlikely that large

https://doi.org/10.1021/acs.iecr.1c03592
Ind. Eng. Chem. Res. XXXX, XXX, XXX−XXX

scale CO_2 electrolyzers will be operated on a discontinuous basis due to the very high capital cost of these processes, which will result in an extremely high payback time. For the base case of the techno-economic analysis, we will assume an electricity price of $25/MWh. The operating costs of the low temperature CO_2 or CO electrolyzers were computed from the power consumption:

$$P_j = i_j A V \tag{3}$$

where P_j is the power required to produce component j, i_j is the partial current density for component i, A is the electrode area, and V is the cell voltage. The electrode area (A) required to convert 10 tons/h of CO_2 was estimated from

$$A = \frac{N_{CO_2}}{(i_t/F)\sum -\nu_j(FE_j/n_j)} \tag{4}$$

where N_{CO_2} is the mole flow of CO_2, i_t is the total current density, F is the Faraday constant, FE_j is the Faraday efficiency for component j, n_j is the number of electrons involved in the CO2R (12, 12, and 8 for ethylene, ethanol, and acetic acid, respectively), and ν_j is the stoichiometric number of CO_2 in the respective CO2R (−2 for ethylene, ethanol, and acetic acid), where the convention is used that reactants have a negative stoichiometric number.

The operating cost of the high temperature SOEC unit was derived from the total energy consumption (6−8 kWh/Nm^3 CO) reported by Haldor Topsoe for CO_2 electrolysis to CO. A value of 6 kWh/Nm^3 CO was used in the economic analysis. The operating cost can then be determined from the required amount of CO, corresponding to the conversion target of 10 tons/h CO_2, and the electricity price. We have assumed that the total energy consumption includes the electrical and thermal energy demands of the SOEC but excludes the energy required for the downstream separation. The energy/cost required for CO_2 separation from the CO product was obtained from the correlation of Bains et al.[98]

It is difficult to estimate the capital cost of CO_2/CO electrolyzers, because there are currently no large scale CO_2/CO electrolyzers available on the market. For this reason, we have estimated the capital cost by comparison with related electrolysis processes. In Table 1, we estimated the capital costs of water electrolyzers (alkaline and SOEC), the chlor-alkali process, and aluminum smelters. For the water electrolyzers, we have used target current densities and capital costs per kilowatt reported by Hydrogen Europe.[103] The capital cost of the chlor-alkali process was estimated in our previous work.[7] Data for aluminum electrolyzers have been taken from the literature.[104−108] Using typical values for the current density and operational voltage of the processes, we have converted the capital cost per unit of power ($/kW) to a capital cost per unit of electrolyzer area ($/$m^2$). For low temperature CO_2 or CO electrolyzers, we have assumed a capital cost of $20,000/$m^2$, which lies between the SOEC and chlor-alkali capital costs. In the absence of commercial scale units, we feel that this cost of merit is justifiable considering the similar complexities and operating conditions of these processes. For the SOEC, we have used a projected cost of €1250/kW reported by Hydrogen Europe.[103]

Table 1. Capital Costs of Water Electrolyzers, Chlor-Alkali Process, and Aluminum Smelters

parameter	unit	AEC	SOEC	chlor-alkali	aluminum
cell voltage	V	2.0	1.5	3.0	4.5
CD	mA/cm^2	600	850	500	1000
power	kW/m^2	12	13	15	45
CAPEX	$/kW	650	1,250	2,000	2,500
CAPEX	$/$m^2$	7,800	15,938	30,000	112,500

The capital and operating costs of the ethanol and acetic acid distillation columns were calculated by Aspen Plus. As utilities, cooling water, low pressure steam, and medium pressure steam were used at a cost of $1.5/GJ, $6.0/GJ, and $8.0/GJ, respectively. The capital cost of the extractor was estimated with the correlations from Woods.[109] The operating cost of the extractor was neglected, because this is typically very small compared to the solvent recovery (acetic acid distillation) column. The capital cost of the five-bed VPSA process was estimated according to the guidelines provided by Woods.[109] The operating cost of the VPSA process is mainly determined by the power consumption of the vacuum pumps and/or compressors. The power input (W) for adiabatic vacuum pumps and compressors for ideal gas can be estimated from[110]

$$W = (n_f/\eta)\left(\frac{\gamma-1}{\gamma}\right)RT_1\left[\left(\frac{P_2}{P_1}\right)^{(\gamma-1)/\gamma} - 1\right] \tag{5}$$

where n_f is the mole flow, η is the compressor/pump efficiency assumed to be 0.7, $\gamma = C_P/C_V$ is the adiabatic expansion coefficient, R is the ideal gas constant, T_1 is the inlet temperature, and P_2/P_1 is the pressure ratio. The capital costs of the vacuum pump and the compressor were estimated from the correlation of Luyben.[111]

The capital costs of the membrane units were estimated using a skid price of $500/$m^2$ membrane area. This cost is based on the works of Baker et al.[112] and includes the cost of membrane modules, module housing, valves, instrumentation, piping, and frame structures. The cost of compressors is not included in the turnkey skid price, but in our process design compressors are not required, since the electrolyzer is operated at high pressure. The required membrane area for the different gas separations was calculated from the countercurrent hollow fiber model of Pettersen and Lien.[91] The details of all these calculations are provided in the Supporting Information (section S2).

The selling prices of products can have a huge effect on the economic analysis. The prices assumed here are based on the European market, which can be very different from U.S. or Middle East prices. For example, the price of ethylene in Europe ($1,200/ton) is almost twice the U.S. price of ethylene. The same holds for the prices of other products such as ethanol and acetic acid, which can differ strongly depending on the region. Therefore, the competitiveness of the electrochemical process will highly depend on the region and market conditions. Also, the grade of the products can have a significant influence on the price. Here, we have designed the downstream process to produce absolute ethanol (>99.5%) and glacial acetic acid (>99.5%), which have much higher market prices compared to the lower grades of the products. Note that the byproduct hydrogen is purified up to 99%, which can be sold to conform to the market price ($1,000/ton). The value of oxygen produced at the anode in the electrolyzers is not taken into account in the economic analysis. However, in

https://doi.org/10.1021/acs.iecr.1c03592
Ind. Eng. Chem. Res. XXXX, XXX, XXX−XXX

the system integration section, we provide guidelines how the produced oxygen can be utilized. Furthermore, we do not consider any premium pricing for the carbon-neutral products. It is obvious that any carbon credits will have a positive impact on the economics of CO_2 utilization processes.

Financial Assumptions. The profitability of a process is often judged on the basis of the payback time (PBT), the return on investment (ROI), or the discounted cash flow, also referred to as the net present value (NPV) approach. Here, we will employ the NPV criteria to evaluate the economic feasibility of the single-step or two-step CO2R/COR processes. The NPV is calculated by taking the sum of the discounted cash flows over the lifetime of the process:

$$\mathrm{NPV} = \sum_{i=0}^{i=n} \frac{C_n}{(1+\mathrm{ir})^n} \tag{6}$$

where C_0 is the initial investment, C_n is the cash flow, n is the year, and ir is the interest rate. We assumed a nominal interest rate of 5% and an income tax rate of 25%. The straight line depreciation method was applied over a depreciation period of 10 years using a salvage value of 10% of the total capital investment at the end of plant life. The working capital was assumed to be 5% of the capital investment, which was recovered at the end of the project. The total CAPEX was calculated as the sum of the capital cost of all units. The yearly profit was calculated from the revenues generated by selling the products minus the annual OPEX of the process. In the economic analysis we have assumed that 1% of all products are lost in the downstream separation process. The lifetime of the process was assumed to be 20 years with 8000 h/year of operation.

Economic Analysis for CO2R to C_2 Products. In this section, we will present the results of the economic analysis for the single-step CO2R process to C_2 products. In Table 2, the capital and operating costs of all the major units are presented. The total capital cost and the operating cost of the CO2R process are around \$180M and \$30M/year, respectively. A breakdown of the CAPEX and OPEX is also shown in Table 2. It is interesting to see that the share of the CO_2 electrolyzer in the CAPEX and OPEX is >80%. Despite the difficult separations, the downstream processing costs are relatively low compared to the electrolyzer costs. The revenues generated from selling the products is approximately \$36M/year. The NPV of the CO2R process is negative, and the payback time is higher than the operational lifetime of the plant. Therefore, the CO2R process is not profitable under the base case conditions considered here. It is clear that the CAPEX and OPEX of the CO_2 electrolyzer need to be reduced drastically to make the process profitable. For the CAPEX this means that a higher current density is required or the capital cost per electrolyzer area (\$/m^2) needs to be reduced. To reduce the OPEX, the power requirement (i.e., the cell voltage) should be reduced or the electricity price should drop significantly.

Table 2. Capital and Operating Costs of the Single-Step CO2R Process

step	CAPEX/\$M	OPEX/(\$M/year)	CAPEX/%	OPEX/%
CO_2 capture	9.5	1.4	5.3	4.7
CO_2 recycling	7.3	1.1	4.0	3.6
LT CO_2 electrolyzer	146.2	25.6	81.1	84.1
C_2H_4 separation	1.8	0.01	1.0	0.0
ethanol separation	7.1	0.7	3.9	2.3
acetic acid separation	8.4	1.6	4.7	5.3
total	180.2	30.4	100.0	100.0

In Figure 3, a sensitivity analysis is performed to show the effects of cell voltage, electricity price, product price, current density, and electrolyzer capital cost on the economics. It is clear that the product price and the electricity price have a strong influence on the economics. A positive NPV can be obtained by reducing the cell voltage to 2.0 V, or by lowering the capital cost of the electrolyzer to <\$3,000/m^2, or by using an electricity price of <\$15/MWh, or by increasing the selling price of all the products by 35%. All these individual targets are very hard to achieve, but the economics can be improved significantly if progress is made on all fronts. For example, the NPV of the process increases to \$38M and a payback time of 13 years is achieved for a cell voltage of 3.0 V, an electricity price of \$20/MWh, and a capital cost of \$10,000/m^2. For the economics, it is important to have a high C_2 selectivity, not necessarily a high ethylene selectivity, because all the CO2R products are valuable and can be sold (after separation) for a relatively high price. To understand this, in Table 3, we have computed the value of 1 mol of supplied electrons (V_e) based on the required number of electrons and the market price of the products:

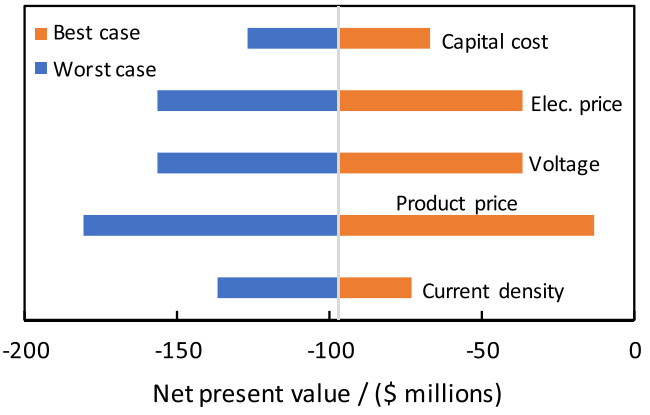

Figure 3. Sensitivity analysis of NPV for the single-step CO_2 reduction to C_2 products. Base case parameters: electrolyzer capital cost, \$20,000/m^2; electricity price, \$25/MWh; cell voltage, 3.5 V; product price \$1,200/ton, \$800/ton, \$800/ton, and \$1,000/ton for ethylene, ethanol, acetic acid, and hydrogen; current density, 500 mA/cm^2; and base case NPV, −\$97M. The best case and worst case scenarios represent an increase or decrease of the base case parameters by 25%.

$$V_e = \frac{P_p M_w}{n} \tag{7}$$

where V_e is in (\$/mol of electrons), P_p is the market price of the product in (\$/g), M_w is the molecular weight in (g/mol), and n is the mole of electrons required to produce 1 mol of product.

The values of V_e for ethylene, ethanol, acetic acid and hydrogen are \$2.8 × 10^{-3}/mol of electrons, \$3.1 × 10^{-3}/mol of electrons, \$6.0 × 10^{-3}/mol of electrons, and \$1.0 × 10^{-3}/

https://doi.org/10.1021/acs.iecr.1c03592
Ind. Eng. Chem. Res. XXXX, XXX, XXX−XXX

Table 3. Value of 1 mol of Electron Input Based on Market Price of the Components

component	n/(e/mol)	M_w/(g/mol)	price[a]/($/ton)	$V_e \times 1{,}000/(\$/e)$
C_2H_4	12	28.05	1,200	2.8
ethanol	12	46.07	800	3.1
acetic acid	8	60.05	800	6.0
hydrogen	2	2.01	1,000	1.0

[a]Prices are based on www.icis.com and www.echemi.com.

mol of electrons, respectively. From this we can conclude that both ethanol and acetic acid are more valuable than ethylene per electron input. On the other hand, hydrogen is almost 3 times less valuable than ethylene. Hence, the coproduction of ethanol and acetic acid will not have a negative impact on the economics of the ethylene process, but hydrogen production should be minimized. In other words, the economics of the ethylene process will not be affected if the sum of the FEs for the C_2 products are high (i.e., a relatively low FE for hydrogen). However, we note that an increase in the FE for ethylene will likely cause a decrease in the FEs of acetic acid and/or ethanol and vice versa. In general, a high FE toward a single product will reduce the separation costs, but the cost reduction will be marginal, because the contribution of the downstream processing to the overall cost is relatively low. This conclusion is somewhat different from those of previous studies,[20,22] which showed a strong dependence of the ethylene price on the FE of ethylene. The main reason for the apparently conflicting conclusion is due to the underlying assumption for the product distribution. Most of these studies assumed ethylene as the only CO2R product with hydrogen as the byproduct. In this case, a decrease in the FE of ethylene automatically results in an increase in the FE of hydrogen. This will affect the economics, because (1) hydrogen is less valuable than ethylene per electron input and (2) often no value is given to the produced hydrogen. In our case, a decrease in the FE of ethylene can be compensated by the increase in the FEs for ethanol and/or acetic acid, while keeping the FE of hydrogen constant. Finally, we note that it is currently not possible to only produce ethylene, since ethanol and acetic acid are coproduced on Cu catalysts. Current research is mainly dedicated to optimizing the catalyst, process conditions, and reactor design for a better selectivity, but there is much to be gained from an optimized separation train. Given the limited number of catalysts that can produce hydrocarbons and the complex multielectron transfer reactions involved, we feel that CO2R or COR to multicarbon products will always yield a mixture of different components. For this reason, it is important to develop efficient downstream processes tailored for the separation of CO2R or COR products.

Economic Analysis for CO2R/COR to C_2 Products. In this section, we will present the results of the economic analysis for the two-step CO2R/COR process to C_2 products. The low temperature CO_2 to CO process will be discussed first and then the high temperature SOEC process. In Table S4, the capital and operating costs of the low temperature process for CO_2 reduction to CO followed by CO electrolysis to C_2 products are presented. The total CAPEX and OPEX of the low temperature two-step process are around $181M and $25M/year, respectively. The electrolyzers contribute approximately >75% to the total CAPEX and OPEX. Revenues generated from selling the products are similar to those in the single-step CO2R process ($36M). The NPV of the low temperature two-step process is negative, which means that the process is not profitable under the base case scenario. However, a positive NPV can be obtained by setting the cell voltage of both electrolyzers to 2.0 V, or by using a capital cost of $10,000/m^2 for both electrolyzers, or by using an electricity price of $15/MWh. Simultaneously reducing the cell voltage of the COR process (2.5 V), the electricity price ($20/MWh), and the capital cost of both electrolyzers ($10,000/m^2) yields a NPV of $67M and a PBT of 10 years. These results show that only slight improvements, but at all fronts, are required to have an economically feasible process.

In Table S5, the capital and operating costs of the high temperature CO2R to CO followed by the low temperature COR process are presented. The total CAPEX and OPEX of the process are around $130M and $24M/year, respectively. Again, the CAPEX and OPEX of the CO_2 and CO electrolyzers have a high share in the total costs. The income from selling the products is approximately $36M. The process has a positive NPV under the base case scenario, but the payback time is 20 years. The NPV increases to $46M (PBT of 13 years), $41M (PBT of 14 years), and $28M (PBT of 15 years) by individually changing the cell voltage to 2 V, using an electricity price of $20/MWh, and lowering the capital cost of the CO electrolyzer to $10,000/m^2, respectively. A NPV of $79M and a PBT of 9 years are obtained by simultaneously reducing the cell voltage (2.5 V), the electricity price ($20/MWh), and the capital cost of the CO electrolyzer ($10,000/m^2). In Figure 4, a sensitivity analysis is performed to show the effects of different parameters on the economics. Again, the product price and electricity price seem to have a huge effect on the economics. It is clear that the high temperature two-

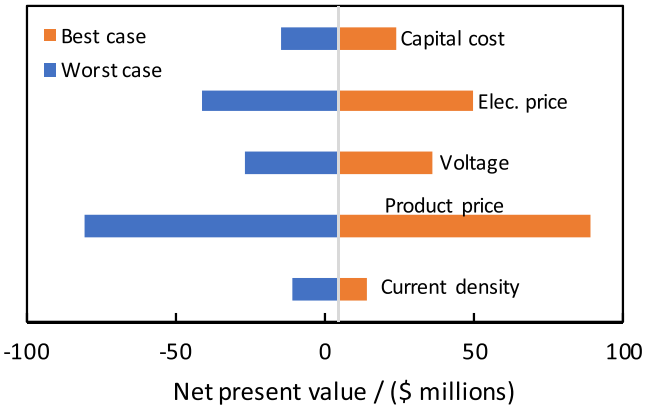

Figure 4. Sensitivity analysis of NPV for the two-step CO_2/CO reduction to C_2 products. Base case parameters: electrolyzer capital cost, $20,000/m^2 for CO electrolyzer and $1,250/kW for SOEC; electricity price, $25/MWh; cell voltage, 3.0 V; product price $1,200/ton, $800/ton, $800/ton, and $1,000/ton for ethylene, ethanol, acetic acid, and hydrogen; current density, 750 mA/cm^2; and base case NPV, $4.5M. The best case and worst case scenarios represent an increase or decrease of the base case parameters by 25%.

https://doi.org/10.1021/acs.iecr.1c03592
Ind. Eng. Chem. Res. XXXX, XXX, XXX−XXX

step process is more profitable than the low temperature two-step process and the single-step CO2R process. The two-step process, in particular the high temperature route, has better technical and economic feasibility compared to the single-step route due to a higher TRL, lower capital cost and operating cost, and higher conversion efficiency and selectivity for C_2 products.

In summary, neither the single-step nor the two-step process is profitable under the base case scenario considered here, but the economics can be improved significantly by reducing the cell voltage, the capital cost of the electrolyzers, and the electricity price. A cell voltage of 2.5 V, a capital cost of \$10,000/m^2, and an electricity price of \$20/MWh will yield a positive NPV and a payback time of less than 15 years for all three conversion processes studied here. Therefore, improvements at all fronts are required to have an economic feasible process that can be scaled up. Future studies should focus on the reduction of the CAPEX and OPEX of the electrolyzers, because these account for >75% of the total cost. Furthermore, we have provided guidelines to separate the complex gaseous and liquid products using currently best available technologies. We have shown that it is not necessary to have a high FE for a single CO2R product (e.g., ethylene), since the coproduced chemicals are also valuable and can be recovered at a relatively low cost. Our analysis shows that the high temperature two-step tandem process is currently the best technology to produce C_2 products. This is in agreement with the conclusions of a number of recent studies.[18,22,51,84]

We have already discussed a couple of options to improve the economics of CO2R or COR to C_2 products. Most of these options require significant technological and/or manufacturing advancements in terms of catalyst/materials development to improve FEs and CDs, reduce cell voltages, reduce power requirements (lower electricity prices), and reduce capital costs of electrolyzers. An interesting way to improve the economics of the overall process is to couple the CO2R/COR at the cathode with an oxidation reaction at the anode that produces a more valuable product than oxygen. Verma et al.[113] showed that the coelectrolysis of CO_2 and glycerol can reduce the electricity consumption by 53%. Recently, Khan et al.[114] demonstrated that the cost of CO2R to ethylene can be reduced by 80% when combined with glycerol oxidation at the anode to produce glycolic acid. These coelectrolysis concepts are very promising, but they will require simultaneous optimization of both reactions, and strategies to prevent product crossover and recovery of products. A more appealing approach to improve the economics is by smart system integration where the CO2R/COR electrolyzer is embedded into an existing manufacturing process. System integration can significantly reduce the CAPEX and OPEX costs of upstream and downstream processes and does not require any additional technological advancement other than catalyst stability. Recently, Barecka et al.[110] showed that it is economically viable to integrate the CO2R unit into an existing ethylene oxide (EO) plant, which had a payback time of 1−2 years in regions with low electricity prices and high carbon taxes. We believe that system integration will play a crucial role in the acceptance and scale-up of CO_2/CO electrolyzers. An example of such an integration was recently presented by van Bavel et al.,[115] who discussed the integration of CO_2 electrolyzers into gas-to-liquid (GTL) and power-to-liquid (PTL) processes.

In the following, guidelines and strategies are presented to smartly integrate CO_2/CO electrolyzers into the existing oil and gas infrastructure. Such an integration will be beneficial in the transition period to avoid the high cost associated with stranded assets.

INTEGRATION OF CO_2/CO ELECTROLYZERS

As explained earlier, it is very unlikely that CO_2/CO electrolyzers will operate on a standalone basis, because (1) the required feedstocks (e.g., CO_2 and electricity) should be available from nearby sources to minimize logistics costs and (2) a range of difficult to handle (gaseous and liquid) products are obtained which requires a costly infrastructure for further processing, storage, transportation, and distribution. Note that difficult to condense or toxic molecules are often directly used on-site at a chemical plant to minimize storage/transportation costs and environmental and safety issues. For these reasons, CO_2/CO electrolyzers should be integrated into the existing infrastructure, which has been unrolled in the past century for the oil and gas industry around the globe. In the following, the best strategies for system integration are analyzed on the basis of feedstock requirements, distribution of products, and process conditions. Considering the feedstocks, CO_2, clean water, and renewable electricity, it would be beneficial to integrate the electrolyzer with readily available CO_2 streams and renewable energy sources (e.g., solar or wind). The products of CO_2/CO electrolysis to C_{2+} products are typically ethylene, acetic acid or ethanol, and oxygen. The aim is to avoid storage and transportation of ethylene by directly converting it to desired easy to handle (liquid) products. Therefore, one option is to integrate the CO_2 electrolyzer into processes that use ethylene as feedstock. Ethylene is mainly used to produce a range of intermediates for the polymer industry, e.g., polyethylene (59%), ethylene oxide (13%), ethylene dichloride (13%), ethylbenzene (7%), and others (8%).

In Table 4, a selection of ethylene-based processes and their operating conditions are reported. The most obvious solution would be to integrate the CO_2/CO electrolyzer into an existing ethylene plant which already has an infrastructure for reactant and product handling. For example, most ethylene plants have a gas removal (CO_2 capture) section and a downstream section to purify ethylene. Additionally, the byproduct hydrogen could easily be used on-site in a refinery, reducing the costs of compression, storage, and transportation. Eliminating the CO_2 capture step and some downstream units will significantly

Table 4. Typical Reaction Conditions of Ethylene-Based Processes[a]

product	P/bar	T/°C	reactants
polyethylene	1500−3500	>160	ethylene
ethylbenzene	40	<289	ethylene, benzene
ethylene oxide	10−30	200−300	ethylene, oxygen
ethylene dichloride	<5	85−200	ethylene, chlorine
ethyl acetate	10	180	ethylene, acetic acid
vinyl acetate	5−12	120−180	ethylene, acetic acid, oxygen
acetaldehyde	4	130	ethylene, oxygen
2-ethoxyethanol	15	150−200	ethylene oxide, ethanol
diethyl ether	<50	<150	ethylene, ethanol
ethanol	50−80	300	ethylene, water

[a]Data taken from refs 116 and 127−134.

https://doi.org/10.1021/acs.iecr.1c03592
Ind. Eng. Chem. Res. XXXX, XXX, XXX−XXX

improve the economics of the electrolysis process. However, based on the product distribution of CO_2/CO electrolyzers and the required reactants and conditions for the processes in Table 4, it is probably better to integrate the electrolysis process within a vinyl acetate (VA) plant. To understand why this is the ideal integration, it is important to first discuss the VA process. VA is produced via the exothermic reaction of ethylene, acetic acid and oxygen over a palladium catalyst:

$$C_2H_4 + CH_3COOH + 0.5O_2 \rightarrow C_4H_6O_2 + H_2O \quad (8)$$

In Figure 5, a typical process flow diagram of a vinyl acetate plant integrated with a CO_2 electrolyzer is shown.[116] The VA process involves the following steps: feed preparation, reaction, phase separation, gas washing and recycling, and product distillation. In the feed preparation step, fresh ethylene, acetic acid, and recycled feed materials are mixed in a 2−3:1 mole ratio of ethylene to acetic acid and preheated to a temperature of 120−180 °C. This mixture is diluted with (recycled) CO_2 (10−30%) to control the exothermicity and explosive limits in the reactor. In a next step, up to 0.5 mol equivalent of oxygen relative to acetic acid and some catalyst promoter (potassium acetate) are added in the stream just before the high pressure reactor. The reactor is operated between 5 and 12 bar, but the conversion of reactants is relatively low due to the low residence time in the reactor to prevent overoxidation. In a subsequent step, the reaction mixture is phase-separated into a gaseous stream mostly containing the unconverted reactants, an organic-rich phase containing the liquid (by)products, and a water-rich phase. The gas stream is treated in a washing column (not shown in Figure 5) to remove traces of acetic acid and (by)products. After the washing step, part of the ethylene and CO_2 mixture is recycled to the feed preparation unit and another part is sent to a CO_2 scrubber to remove excess CO_2 formed due to side reactions in the reactor. The organic-rich phase, containing 20−40% vinyl acetate, >50% acetic acid, 6−10% water, and small amounts of byproducts (e.g., ethyl acetate), is sent to an azeotropic distillation column. VA and water form a low-boiling heterogeneous azeotrope and leave the column as distillate, while acetic acid is recovered as bottoms and recycled back to the feed preparation step. The distillate is condensed into a water-rich stream and a vinyl acetate rich stream, which is further purified in a product distillation column (not shown in Figure 5).

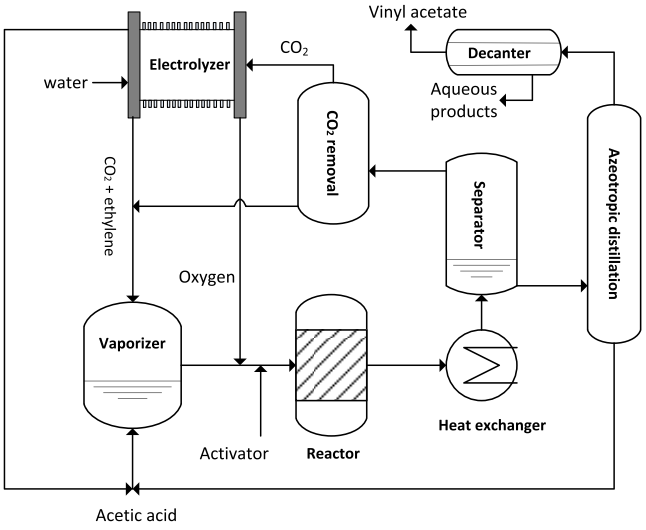

Figure 5. Integration of a CO_2 electrolyzer into the vinyl acetate (VA) process. CO_2 produced in the VA process or from other sources are fed to the electrolyzer, which produces ethylene and acetic acid at the cathode and oxygen at the anode. These electrolysis products, together with the unconverted CO_2, are mixed in the vaporizer and fed to the high pressure reactor, which operates at 120−180 °C and 5−12 bar. After the reaction mixture is cooled, the gaseous and liquid streams are separated. The gaseous stream is washed to remove traces of liquid products (washing step not shown) and sent to a CO_2 capture unit, which removes additional CO_2 produced in the reactor due to overoxidation of ethylene. The liquid products from the separator is fed to the azeotropic distillation column, where acetic acid is recovered as bottoms and recycled back to the vaporizer. The azeotropic mixture of vinyl acetate and water azeotrope leaves the column as tops and is condensed in a decanter into a VA-rich stream and an aqueous stream. Both streams might be purified further, but this is not shown in the diagram.

The integration of the CO_2-to-ethylene electrolyzer into the VA process is ideal, because (1) the electrolyzer produces ethylene and acetic acid in a ratio similar to that desired in the VA process; (2) the gas stream from the electrolyzer contains ethylene and unconverted CO_2, which can directly be fed to the VA process; (3) the pure oxygen produced at the anode can be used in the VA reactor, which eliminates the need for an air separation unit; (4) the excess CO_2 and water produced in the VA process can be utilized in the CO_2 electrolyzer; (5) the VA process already has CO_2 capture and distillation units, which will simplify retrofitting of the CO_2 electrolyzer; and (6) multiple gaseous feedstocks are converted to a single relatively easy to handle liquid product, which simplifies storage and transportation. Furthermore, it is beneficial to operate the electrolyzer at slightly elevated temperatures and pressures to match the conditions of the VA process. In addition, the current density and CO_2 conversion in the electrolyzer are higher for elevated temperature and pressure conditions. Furthermore, it is beneficial to use a three-compartment alkaline CO_2 electrolyzer, since acetic acid and not acetate is required as feedstock in the VA process.

In the previous integration example, we have assumed that acetic acid is the main byproduct of CO2R. However, it is clear that the system integration will be different for ethanol as the main byproduct, but the strategy is again to convert ethylene to some liquid products. In Table 4, different options for integrating the CO_2/CO electrolyzer into ethylene- or ethanol-based processes are provided. The first option is to convert ethylene to ethylene oxide, which can subsequently be reacted with ethanol to produce 2-ethoxyethanol. The second option is to react ethylene and ethanol to produce diethyl ether. The third option is to convert ethylene to ethanol, but this route seems to be economically less attractive compared to the fermentation process. Of course, ethylene can be transformed to any other products mentioned in Table 4 but not involving ethanol in the reaction. In the latter case, two liquid products will be produced in the integrated process, which is not an issue as long as the existing infrastructure can be used.

The above proposed integration is based on the assumption that CO_2 is the reactant (i.e., single-step CO2R), which results in a CO_2 and ethylene mixture for conversions lower than 100%. However, in the two-step process (i.e., CO2R/COR), CO is the reactant, which will yield a mixture of CO and ethylene for incomplete conversions. An option in this case is to integrate the CO electrolyzer into a propionic acid plant for

https://doi.org/10.1021/acs.iecr.1c03592
Ind. Eng. Chem. Res. XXXX, XXX, XXX−XXX

the hydrocarboxylation of ethylene according to the reaction[117]

$$C_2H_4 + CO + H_2O \rightarrow CH_3CH_2COOH \quad (9)$$

One of the main byproducts in COR is ethanol, which can be converted with ethylene and CO to ethyl propionate by essentially replacing water by ethanol in eq 9. Clearly, the system integration will be affected by the choice of the conversion process (i.e., CO2R or COR) and the formed byproducts.

For the system integration, we have selected processes on the basis of the typical product distributions of CO2R and COR electrolyzers, the reaction temperature and pressure conditions, and the required reactants. However, the integration might also depend on the location, the availability of feedstocks, the desired purity of products, the operational flexibility and reliability of renewable energy based processes, and the costs of retrofits. Since there are a couple of options for system integration, the ultimate decision can only be made after a detailed techno-economic analysis of the fully integrated system, which is beyond the scope of the current work. Nevertheless, we hope that the basic strategies presented here will help to accelerate the commercialization of CO_2/CO electrolyzers. Furthermore, the strategies presented here are also applicable to other gaseous CO_2 electroreduction products such as CO and methane. It is clear that decentralized production of gaseous products will bring additional expenses for transport and storage, which can be avoided when CO_2 electrolyzers are smartly integrated into the existing infrastructure. Such an integration will be crucial for the large scale implementation of power-to-X concepts including CO_2 electrolysis to value-added products. In the next section, we present a list of current barriers that impede scale-up and commercialization of CO_2 electrolyzers. These barriers were partly derived from the carbon capture and storage (CCS) field,[118−122] but they apply equally well to carbon capture and utilization (CCU)[123−125] and were partly identified during the Energy-X workshop "research needs: toward sustainable production of fuels and chemicals" in Brussels (Belgium).[126]

BARRIERS FOR INDUSTRIALIZATION OF CO_2 ELECTROLYZERS

Often, it takes a lot of effort, time, and persistence to replace well-established (fossil fuel based) processes with new (renewable energy based) technologies. To accelerate the implementation of CO_2 electrolyzers in the chemical industry, the following barriers need to be addressed.

1. Lack of upstream and downstream processing studies: The effect of impurities in the reactants and products has rarely been investigated, but it is well-known that upstream and downstream purification steps can account for >30% of the total costs. It is obvious that the feedstock costs will be significantly higher if ultrapure CO_2 and water are required in the electrolysis process.

2. Lack of system integration studies: As explained earlier, it is very unlikely that CO_2 electrolyzers will operate on a standalone basis due to the lack of infrastructure. It is better to integrate CO_2 electrolyzers into the existing fossil fuel based infrastructure. However, it is currently unclear how to retrofit CO_2 electrolyzers into chemical processes.

3. Lack of process design and techno-economic feasibility studies: It is important to consider the economics of a new technology in an early stage of the development process to assess the competitiveness, select the most promising alternatives, and identify research and development gaps.

4. Lack of scale-up studies: For new technologies, it is common practice to first run long-term pilot scale experiments before implementing on a commercial scale. To assess the feasibility of CO_2 electrolysis at an industrial scale, it is important to move from lab to pilot scale.

5. Lack of infrastructure: Power-to-X concepts such as CO_2 electrolysis require an infrastructure for the feedstocks (e.g., renewable energy and CO_2) and products. The lack of such an infrastructure is a significant barrier for scale-up and industrialization of CO_2 electrolyzers.

6. Lack of funding opportunities: Development of new technologies requires a high up-front investment, which is one of the main hurdles for start-up companies to bringing the product on the market. This initial investment should come from fund-raising, because major companies are typically reluctant to invest in low TRL technologies.

7. Lack of regulations and policy incentives for large scale CCU projects: Currently, it is extremely difficult for CCU processes to economically compete with the fossil fuel based counterparts. In the absence of direct economic drivers, a clear regulatory framework and policy incentives are crucial for successful implementation of CCU projects on a large scale.

8. Lack of environmental, health and safety, and societal impact studies: A large number of CCS projects have been canceled due to underestimation of ecological and societal factors such as public acceptance. To avoid similar issues with CCU, it is important to thoroughly assess the impact of new technologies on the environment and society and to involve all stakeholders at an early stage of the development.

9. Lack of education and training: A large amount of manpower with skills in power-to-X technologies will be required for the envisioned large scale deployment of CO_2 electrolyzers. The new generation of operators, technicians, and engineers needs to be educated and trained for the operation of renewable energy based processes.

By adequately addressing these barriers, we might be able to accelerate the implementation of power-to-X technologies including CO_2 electrolyzers on an industrial scale. However, experience from the CCS field shows that a significant effort from all stakeholders (i.e., energy companies, industry, policy makers, technology suppliers, environmental agencies, local public, nongovernmental organizations, and academia) will be required to make a success of CCU.

CONCLUSIONS

Direct electrochemical reduction of CO_2 to value-added products (i.e., the single-step process) is more efficient is alkaline conditions, but it has a negative impact on the carbon utilization due to (bi)carbonate formation. A two-step (tandem) process, where CO_2 is first converted to CO which is then further reduced to the desired products (indirect route), has been proposed to overcome the problems associated with direct CO_2 conversion in alkaline media. Here, we performed a detailed process design and techno-economic analysis for direct and indirect CO_2 conversion to C_2 products (ethylene, acetic acid, and ethanol). For the two-step tandem process, CO production by high temperature (i.e., SOEC) or low temperature CO_2 electrolysis has been considered in the design. For both (CO2R and CO2R/COR) processes, guidelines are provided for the downstream processing of the complex gas and liquid mixtures containing

https://doi.org/10.1021/acs.iecr.1c03592
Ind. Eng. Chem. Res. XXXX, XXX, XXX−XXX

CO_2, ethylene, CO, H_2, acetic acid, and ethanol. Process modeling and economic analysis of both (single-step and two-step) routes have been performed. Capital and operating costs of CO_2 capture, CO_2/CO reduction, CO_2 recycling, and product separation have been calculated for both routes. Our economic analysis shows that with the current electrolyzer performance, electricity prices, and electrolyzer capital costs both routes are economically not compelling. However, the economics of both processes can be improved significantly by reducing the CAPEX and OPEX of the electrolyzers, which have a high share (>75%) in the total cost. For both routes, a cell voltage of <2.5 V, an electricity price of <$20/MWh, and a capital cost of <$10,000/$m^2$ for the electrolyzers will result in a significantly improved economics (NPV of >$60M and payback times between 9 and 11 years). We demonstrate that the coproduction of ethanol and acetic acid does not have a negative impact on the economics of the process, because the downstream separation costs are relatively low and both products can be sold for a high market price. For this reason, it is not necessary to have a high FE for a single product, but it is crucial to keep the sum of the FEs for the C_2 products high. Overall, the high temperature two-step tandem process has a better technical and economic viability than the single-step CO2R process and the low temperature two-step process. Guidelines are provided to integrate CO_2/CO electrolyzers into the existing oil and gas infrastructure, which will be crucial to increasing the acceptance of these technologies, to reducing upstream and downstream processing costs, and to avoiding problems with logistics, storage, transportation, and distribution of difficult to handle gaseous and liquid products. Finally, we provide an overview of the current barriers that impede commercialization of CO_2/CO electrolyzers.

■ ASSOCIATED CONTENT

Supporting Information

The Supporting Information is available free of charge at https://pubs.acs.org/doi/10.1021/acs.iecr.1c03592.

Data compilation for CO_2 electrolysis to CO and C_2 products; data compilation of CO electrolysis to C_2 products; capital and operating cost estimations for low and high temperature two-step tandem processes; details of modeling of the membrane, VPSA, and extraction/distillation processes; estimation of concentrations of liquid products; and estimation of CO_2 loss to (bi)carbonates (PDF)

■ AUTHOR INFORMATION

Corresponding Author

Mahinder Ramdin − *Engineering Thermodynamics, Process & Energy Department, Faculty of Mechanical, Maritime and Materials Engineering, Delft University of Technology, 2628CB Delft, The Netherlands;* orcid.org/0000-0002-8476-7035; Email: m.ramdin@tudelft.nl

Authors

Bert De Mot − *Applied Electrochemistry & Catalysis, University of Antwerp, 2610 Wilrijk, Belgium;* orcid.org/0000-0002-8510-7960

Andrew R. T. Morrison − *Large-Scale Energy Storage, Process & Energy Department, Faculty of Mechanical, Maritime and Materials Engineering, Delft University of Technology, 2628CB Delft, The Netherlands*

Tom Breugelmans − *Applied Electrochemistry & Catalysis, University of Antwerp, 2610 Wilrijk, Belgium;* orcid.org/0000-0001-5538-0408

Leo J. P. van den Broeke − *Engineering Thermodynamics, Process & Energy Department, Faculty of Mechanical, Maritime and Materials Engineering, Delft University of Technology, 2628CB Delft, The Netherlands*

J. P. Martin Trusler − *Imperial College London, South Kensington Campus, London SW7 2AZ, United Kingdom;* orcid.org/0000-0002-6403-2488

Ruud Kortlever − *Large-Scale Energy Storage, Process & Energy Department, Faculty of Mechanical, Maritime and Materials Engineering, Delft University of Technology, 2628CB Delft, The Netherlands;* orcid.org/0000-0001-9412-7480

Wiebren de Jong − *Large-Scale Energy Storage, Process & Energy Department, Faculty of Mechanical, Maritime and Materials Engineering, Delft University of Technology, 2628CB Delft, The Netherlands*

Othonas A. Moultos − *Engineering Thermodynamics, Process & Energy Department, Faculty of Mechanical, Maritime and Materials Engineering, Delft University of Technology, 2628CB Delft, The Netherlands;* orcid.org/0000-0001-7477-9684

Penny Xiao − *Department of Chemical Engineering, The University of Melbourne, Victoria 3010, Australia*

Paul A. Webley − *Department of Chemical Engineering, Monash University, Victoria 3800, Australia;* orcid.org/0000-0003-3598-3767

Thijs J. H. Vlugt − *Engineering Thermodynamics, Process & Energy Department, Faculty of Mechanical, Maritime and Materials Engineering, Delft University of Technology, 2628CB Delft, The Netherlands;* orcid.org/0000-0003-3059-8712

Complete contact information is available at: https://pubs.acs.org/10.1021/acs.iecr.1c03592

Notes

The authors declare no competing financial interest.

■ ACKNOWLEDGMENTS

T.J.H.V. acknowledges NWO-CW (Chemical Sciences) for a VICI grant.

■ REFERENCES

(1) Nitopi, S.; Bertheussen, E.; Scott, S. B.; Liu, X.; Engstfeld, A. K.; Horch, S.; Seger, B.; Stephens, I. E. L.; Chan, K.; Hahn, C.; Nørskov, J. K.; Jaramillo, T. F.; Chorkendorff, I. Progress and Perspectives of Electrochemical CO_2 Reduction on Copper in Aqueous Electrolyte. *Chem. Rev.* **2019**, *119*, 7610−7672.

(2) Jin, S.; Hao, Z.; Zhang, K.; Yan, Z.; Chen, J. Advances and Challenges for the Electrochemical Reduction of CO_2 to CO: From Fundamentals to Industrialization. *Angew. Chem., Int. Ed.* **2021**, *60*, 20627−20648.

(3) Masel, R. I.; Liu, Z.; Yang, H.; Kaczur, J. J.; Carrillo, D.; Ren, S.; Salvatore, D.; Berlinguette, C. P. An industrial perspective on catalysts for low-temperature CO_2 electrolysis. *Nat. Nanotechnol.* **2021**, *16*, 118−128.

(4) Hori, Y. Electrochemical CO_2 Reduction on Metal Electrodes. In *Modern Aspects of Electrochemistry*; Vayenas, C. G., White, R. E., Gamboa-Aldeco, M. E., Eds.; Springer: New York, NY, 2008; Vol. *42*; pp 89−189..

(5) Jeng, E.; Jiao, F. Investigation of CO_2 single-pass conversion in a flow electrolyzer. *React. Chem. Eng.* **2020**, *5*, 1768−1775.

https://doi.org/10.1021/acs.iecr.1c03592
Ind. Eng. Chem. Res. XXXX, XXX, XXX−XXX

(6) Hitchcock, L. B.; Cadot, H. M. Rate of Absorption of Carbon Dioxide Effect of Concentration and Viscosity of Normal Carbonate Solutions. *Ind. Eng. Chem.* **1935**, *27*, 728−732.
(7) Ramdin, M.; Morrison, A. R. T.; de Groen, M.; van Haperen, R.; de Kler, R.; Irtem, E.; Laitinen, A. T.; van den Broeke, L. J. P.; Breugelmans, T.; Trusler, J. P. M.; Jong, W. D.; Vlugt, T. J. H. High-Pressure Electrochemical Reduction of CO_2 to Formic Acid/Formate: Effect of pH on the Downstream Separation Process and Economics. *Ind. Eng. Chem. Res.* **2019**, *58*, 22718−22740.
(8) Ooka, H.; Figueiredo, M. C.; Koper, M. T. M. Competition between Hydrogen Evolution and Carbon Dioxide Reduction on Copper Electrodes in Mildly Acidic Media. *Langmuir* **2017**, *33*, 9307−9313.
(9) Bondue, C. J.; Graf, M.; Goyal, A.; Koper, M. T. M. Suppression of Hydrogen Evolution in Acidic Electrolytes by Electrochemical CO_2 Reduction. *J. Am. Chem. Soc.* **2021**, *143*, 279−285.
(10) Huang, J. E.; Li, F.; Ozden, A.; Sedighian Rasouli, A.; García de Arquer, F. P.; Liu, S.; Zhang, S.; Luo, M.; Wang, X.; Lum, Y.; Xu, Y.; Bertens, K.; Miao, R. K.; Dinh, C.-T.; Sinton, D.; Sargent, E. H. CO_2 electrolysis to multicarbon products in strong acid. *Science* **2021**, *372*, 1074−1078.
(11) Kaczur, J. J.; Yang, H.; Liu, Z.; Sajjad, S. D.; Masel, R. I. Carbon Dioxide and Water Electrolysis Using New Alkaline Stable Anion Membranes. *Front. Chem.* **2018**, *6*, 263.
(12) Lees, E. W.; Goldman, M.; Fink, A. G.; Dvorak, D. J.; Salvatore, D. A.; Zhang, Z.; Loo, N. W. X.; Berlinguette, C. P. Electrodes Designed for Converting Bicarbonate into CO. *ACS Energy Lett.* **2020**, *5*, 2165−2173.
(13) Li, Y. C.; Lee, G.; Yuan, T.; Wang, Y.; Nam, D.-H.; Wang, Z.; García de Arquer, F. P.; Lum, Y.; Dinh, C.-T.; Voznyy, O.; Sargent, E. H. CO_2 Electroreduction from Carbonate Electrolyte. *ACS Energy Lett.* **2019**, *4*, 1427−1431.
(14) Li, T.; Lees, E. W.; Goldman, M.; Salvatore, D. A.; Weekes, D. M.; Berlinguette, C. P. Electrolytic Conversion of Bicarbonate into CO in a Flow Cell. *Joule* **2019**, *3*, 1487−1497.
(15) Lee, G.; Li, Y. C.; Kim, J.-Y.; Peng, T.; Nam, D.-H.; Sedighian Rasouli, A.; Li, F.; Luo, M.; Ip, A. H.; Joo, Y.-C.; Sargent, E. H. Electrochemical upgrade of CO_2 from amine capture solution. *Nat. Energy* **2021**, *6*, 46−53.
(16) Jouny, M.; Hutchings, G. S.; Jiao, F. Carbon monoxide electroreduction as an emerging platform for carbon utilization. *Nat. Catal.* **2019**, *2*, 1062−1070.
(17) Fu, X.; Zhang, J.; Kang, Y. Electrochemical reduction of CO_2 towards multi-carbon products via a two-step process. *React. Chem. Eng.* **2021**, *6*, 612−628.
(18) Overa, S.; Feric, T. G.; Park, A.-H. A.; Jiao, F. Tandem and Hybrid Processes for Carbon Dioxide Utilization. *Joule* **2021**, *5*, 8−13.
(19) Gurudayal; Perone, D.; Malani, S.; Lum, Y.; Haussener, S.; Ager, J. W. Sequential Cascade Electrocatalytic Conversion of Carbon Dioxide to C−C Coupled Products. *ACS Appl. Energy Mater.* **2019**, *2*, 4551−4559.
(20) Jouny, M.; Luc, W.; Jiao, F. General Techno-Economic Analysis of CO_2 Electrolysis Systems. *Ind. Eng. Chem. Res.* **2018**, *57*, 2165−2177.
(21) Spurgeon, J. M.; Kumar, B. A comparative technoeconomic analysis of pathways for commercial electrochemical CO_2 reduction to liquid products. *Energy Environ. Sci.* **2018**, *11*, 1536−1551.
(22) Sisler, J.; Khan, S.; Ip, A. H.; Schreiber, M. W.; Jaffer, S. A.; Bobicki, E. R.; Dinh, C.-T.; Sargent, E. H. Ethylene Electrosynthesis: A Comparative Techno-economic Analysis of Alkaline vs Membrane Electrode Assembly vs CO_2-CO-C_2H_4 Tandems. *ACS Energy Lett.* **2021**, *6*, 997−1002.
(23) Pappijn, C. A. R.; Ruitenbeek, M.; Reyniers, M.-F.; Van Geem, K. M. Challenges and Opportunities of Carbon Capture and Utilization: Electrochemical Conversion of CO_2 to Ethylene. *Front. Energy Res.* **2020**, *8*, 557466.
(24) Somoza-Tornos, A.; Guerra, O. J.; Crow, A. M.; Smith, W. A.; Hodge, B.-M. Process modeling, techno-economic assessment, and life cycle assessment of the electrochemical reduction of CO_2: a review. *iScience* **2021**, *24*, 102813.
(25) Na, J.; Seo, B.; Kim, J.; Lee, C. W.; Lee, H.; Hwang, Y. J.; Min, B. K.; Lee, D. K.; Oh, H.-S.; Lee, U. General technoeconomic analysis for electrochemical coproduction coupling carbon dioxide reduction with organic oxidation. *Nat. Commun.* **2019**, *10*, 5193.
(26) De Luna, P.; Hahn, C.; Higgins, D.; Jaffer, S. A.; Jaramillo, T. F.; Sargent, E. H. What would it take for renewably powered electrosynthesis to displace petrochemical processes? *Science* **2019**, *364*, No. eaav3506.
(27) Shin, H.; Hansen, K. U.; Jiao, F. Techno-economic assessment of low-temperature carbon dioxide electrolysis. *Nat. Sustain.* **2021**, *4*, 911−919.
(28) Orella, M. J.; Brown, S. M.; Leonard, M. E.; Román-Leshkov, Y.; Brushett, F. R. A General Technoeconomic Model for Evaluating Emerging Electrolytic Processes. *Energy Technol.* **2020**, *8*, 1900994.
(29) Hori, Y.; Kikuchi, K.; Murata, A.; Suzuki, S. Production of methane and ethylene in electrochemical reduction of carbon dioxide at copper electrode in aqueous hydrogencarbonate solution. *Chem. Lett.* **1986**, *15*, 897−898.
(30) Hori, Y.; Murata, A.; Takahashi, R.; Suzuki, S. Electroreduction of carbon monoxide to methane and ethylene at a copper electrode in aqueous solutions at ambient temperature and pressure. *J. Am. Chem. Soc.* **1987**, *109*, 5022−5023.
(31) García de Arquer, F. P.; Dinh, C.-T.; Ozden, A.; Wicks, J.; McCallum, C.; Kirmani, A. R.; Nam, D.-H.; Gabardo, C.; Seifitokaldani, A.; Wang, X.; Li, Y. C.; Li, F.; Edwards, J.; Richter, L. J.; Thorpe, S. J.; Sinton, D.; Sargent, E. H. CO_2 electrolysis to multicarbon products at activities greater than 1 A cm^{-2}. *Science* **2020**, *367*, 661−666.
(32) Dinh, C.-T.; Burdyny, T.; Kibria, M. G.; Seifitokaldani, A.; Gabardo, C. M.; García de Arquer, F. P.; Kiani, A.; Edwards, J. P.; De Luna, P.; Bushuyev, O. S.; Zou, C.; Quintero-Bermudez, R.; Pang, Y.; Sinton, D.; Sargent, E. H. CO_2 electroreduction to ethylene via hydroxide-mediated copper catalysis at an abrupt interface. *Science* **2018**, *360*, 783−787.
(33) De Gregorio, G. L.; Burdyny, T.; Loiudice, A.; Iyengar, P.; Smith, W. A.; Buonsanti, R. Facet-Dependent Selectivity of Cu Catalysts in Electrochemical CO_2 Reduction at Commercially Viable Current Densities. *ACS Catal.* **2020**, *10*, 4854−4862.
(34) Hoang, T. T. H.; Verma, S.; Ma, S.; Fister, T. T.; Timoshenko, J.; Frenkel, A. I.; Kenis, P. J. A.; Gewirth, A. A. Nanoporous Copper−Silver Alloys by Additive-Controlled Electrodeposition for the Selective Electroreduction of CO_2 to Ethylene and Ethanol. *J. Am. Chem. Soc.* **2018**, *140*, 5791−5797.
(35) Vennekötter, J.-B.; Scheuermann, T.; Sengpiel, R.; Wessling, M. The electrolyte matters: Stable systems for high rate electrochemical CO_2 reduction. *J. CO2 Util.* **2019**, *32*, 202−213.
(36) Wang, X.; Wang, Z.; García de Arquer, F. P.; Dinh, C.-T.; Ozden, A.; Li, Y. C.; Nam, D.-H.; Li, J.; Liu, Y.-S.; Wicks, J.; Chen, Z.; Chi, M.; Chen, B.; Wang, Y.; Tam, J.; Howe, J. Y.; Proppe, A.; Todorović, P.; Li, F.; Zhuang, T.-T.; Gabardo, C. M.; Kirmani, A. R.; McCallum, C.; Hung, S.-F.; Lum, Y.; Luo, M.; Min, Y.; Xu, A.; O'Brien, C. P.; Stephen, B.; Sun, B.; Ip, A. H.; Richter, L. J.; Kelley, S. O.; Sinton, D.; Sargent, E. H. Efficient electrically powered CO_2-to-ethanol via suppression of deoxygenation. *Nat. Energy* **2020**, *5*, 478−486.
(37) Zhong, M.; Tran, K.; Min, Y.; Wang, C.; Wang, Z.; Dinh, C.-T.; De Luna, P.; Yu, Z.; Rasouli, A. S.; Brodersen, P.; Sun, S.; Voznyy, O.; Tan, C.-S.; Askerka, M.; Che, F.; Liu, M.; Seifitokaldani, A.; Pang, Y.; Lo, S.-C.; Ip, A.; Ulissi, Z.; Sargent, E. H. Accelerated discovery of CO_2 electrocatalysts using active machine learning. *Nature* **2020**, *581*, 178−183.
(38) Chen, X.; Chen, J.; Alghoraibi, N. M.; Henckel, D. A.; Zhang, R.; Nwabara, U. O.; Madsen, K. E.; Kenis, P. J. A.; Zimmerman, S. C.; Gewirth, A. A. Electrochemical CO_2-to-ethylene conversion on polyamine-incorporated Cu electrodes. *Nat. Catal.* **2021**, *4*, 20−27.
(39) Li, F.; Thevenon, A.; Rosas-Hernández, A.; Wang, Z.; Li, Y.; Gabardo, C. M.; Ozden, A.; Dinh, C. T.; Li, J.; Wang, Y.; Edwards, J.

https://doi.org/10.1021/acs.iecr.1c03592
Ind. Eng. Chem. Res. XXXX, XXX, XXX−XXX

P.; Xu, Y.; McCallum, C.; Tao, L.; Liang, Z.-Q.; Luo, M.; Wang, X.; Li, H.; O'Brien, C. P.; Tan, C.-S.; Nam, D.-H.; Quintero-Bermudez, R.; Zhuang, T.-T.; Li, Y. C.; Han, Z.; Britt, R. D.; Sinton, D.; Agapie, T.; Peters, J. C.; Sargent, E. H. Molecular tuning of CO_2-to-ethylene conversion. *Nature* **2020**, *577*, 509−513.

(40) Ma, W.; Xie, S.; Liu, T.; Fan, Q.; Ye, J.; Sun, F.; Jiang, Z.; Zhang, Q.; Cheng, J.; Wang, Y. Electrocatalytic reduction of CO_2 to ethylene and ethanol through hydrogen-assisted C−C coupling over fluorine-modified copper. *Nat. Catal.* **2020**, *3*, 478−487.

(41) Ozden, A.; Li, F.; Garcia de Arquer, F. P.; Rosas-Hernández, A.; Thevenon, A.; Wang, Y.; Hung, S.-F.; Wang, X.; Chen, B.; Li, J.; Wicks, J.; Luo, M.; Wang, Z.; Agapie, T.; Peters, J. C.; Sargent, E. H.; Sinton, D. High-Rate and Efficient Ethylene Electrosynthesis Using a Catalyst/Promoter/Transport Layer. *ACS Energy Lett.* **2020**, *5*, 2811−2818.

(42) She, X.; Zhang, T.; Li, Z.; Li, H.; Xu, H.; Wu, J. Tandem Electrodes for Carbon Dioxide Reduction into C2+ Products at Simultaneously High Production Efficiency and Rate. *Cell Reports Phys. Sci.* **2020**, *1*, 100051.

(43) Tan, Y. C.; Lee, K. B.; Song, H.; Oh, J. Modulating Local CO_2 Concentration as a General Strategy for Enhancing C-C Coupling in CO_2 Electroreduction. *Joule* **2020**, *4*, 1104−1120.

(44) Wang, Y.; Wang, Z.; Dinh, C.-T.; Li, J.; Ozden, A.; Golam Kibria, M.; Seifitokaldani, A.; Tan, C.-S.; Gabardo, C. M.; Luo, M.; Zhou, H.; Li, F.; Lum, Y.; McCallum, C.; Xu, Y.; Liu, M.; Proppe, A.; Johnston, A.; Todorovic, P.; Zhuang, T.-T.; Sinton, D.; Kelley, S. O.; Sargent, E. H. Catalyst synthesis under CO_2 electroreduction favours faceting and promotes renewable fuels electrosynthesis. *Nat. Catal.* **2020**, *3*, 98−106.

(45) Romero Cuellar, N.; Wiesner-Fleischer, K.; Fleischer, M.; Rucki, A.; Hinrichsen, O. Advantages of CO over CO_2 as reactant for electrochemical reduction to ethylene, ethanol and n-propanol on gas diffusion electrodes at high current densities. *Electrochim. Acta* **2019**, *307*, 164−175.

(46) Romero Cuellar, N.; Scherer, C.; Kaçkar, B.; Eisenreich, W.; Huber, C.; Wiesner-Fleischer, K.; Fleischer, M.; Hinrichsen, O. Two-step electrochemical reduction of CO_2 towards multi-carbon products at high current densities. *J. CO2 Util.* **2020**, *36*, 263−275.

(47) Jouny, M.; Luc, W.; Jiao, F. High-rate electroreduction of carbon monoxide to multi-carbon products. *Nat. Catal.* **2018**, *1*, 748−755.

(48) Jouny, M.; Lv, J.-J.; Cheng, T.; Ko, B. H.; Zhu, J.-J.; Goddard, W. A.; Jiao, F. Formation of carbon−nitrogen bonds in carbon monoxide electrolysis. *Nat. Chem.* **2019**, *11*, 846−851.

(49) Li, J.; Wang, Z.; McCallum, C.; Xu, Y.; Li, F.; Wang, Y.; Gabardo, C. M.; Dinh, C.-t.; Zhuang, T.-t.; Wang, L.; Howe, J. Y.; Ren, Y.; Sargent, E. H.; Sinton, D. Constraining CO coverage on copper promotes high-efficiency ethylene electroproduction. *Nat. Catal.* **2019**, *2*, 1124−1131.

(50) Luc, W.; Fu, X.; Shi, J.; Lv, J.-J.; Jouny, M.; Ko, B. H.; Xu, Y.; Tu, Q.; Hu, X.; Wu, J.; Yue, Q.; Liu, Y.; Jiao, F.; Kang, Y. Two-dimensional copper nanosheets for electrochemical reduction of carbon monoxide to acetate. *Nat. Catal.* **2019**, *2*, 423−430.

(51) Ozden, A.; Wang, Y.; Li, F.; Luo, M.; Sisler, J.; Thevenon, A.; Rosas-Hernández, A.; Burdyny, T.; Lum, Y.; Yadegari, H.; Agapie, T.; Peters, J. C.; Sargent, E. H.; Sinton, D. Cascade CO_2 electroreduction enables efficient carbonate-free production of ethylene. *Joule* **2021**, *5*, 706−719.

(52) Ren, S.; Fink, A.; Lees, E.; Zhang, Z.; Wu, W. Y.; Dvorak, D. J.; Berlinguette, C. Molecular electrocatalysts transform CO into C2+ products effectively in a flow cell [preprint]. *Researchsquare.com*, October 16, 2020. DOI: 10.21203/rs.3.rs-83176/v1.

(53) Ripatti, D. S.; Veltman, T. R.; Kanan, M. W. Carbon Monoxide Gas Diffusion Electrolysis that Produces Concentrated C_2 Products with High Single-Pass Conversion. *Joule* **2019**, *3*, 240−256.

(54) Zhu, P.; Xia, C.; Liu, C.-Y.; Jiang, K.; Gao, G.; Zhang, X.; Xia, Y.; Lei, Y.; Alshareef, H. N.; Senftle, T. P.; Wang, H. Direct and continuous generation of pure acetic acid solutions via electrocatalytic carbon monoxide reduction. *Proc. Natl. Acad. Sci. U. S. A.* **2021**, *118*, No. e2010868118.

(55) Xia, R.; Lv, J.-J.; Ma, X.; Jiao, F. Enhanced multi-carbon selectivity via CO electroreduction approach. *J. Catal.* **2021**, *398*, 185−191.

(56) Gao, D.; Arán-Ais, R. M.; Jeon, H. S.; Roldan Cuenya, B. Rational catalyst and electrolyte design for CO2 electroreduction towards multicarbon products. *Nat. Catal.* **2019**, *2*, 198−210.

(57) Fan, L.; Xia, C.; Yang, F.; Wang, J.; Wang, H.; Lu, Y. Strategies in catalysts and electrolyzer design for electrochemical CO_2 reduction toward C2+ products. *Sci. Adv.* **2020**, *6*, No. eaay3111.

(58) Merino-Garcia, I.; Albo, J.; Irabien, A. Tailoring gas-phase CO_2 electroreduction selectivity to hydrocarbons at Cu nanoparticles. *Nanotechnology* **2018**, *29*, 014001.

(59) Merino-Garcia, I.; Albo, J.; Solla-Gullón, J.; Montiel, V.; Irabien, A. Cu oxide/ZnO-based surfaces for a selective ethylene production from gas-phase CO_2 electroconversion. *J. CO2 Util.* **2019**, *31*, 135−142.

(60) Wang, X.; de Araújo, J. F.; Ju, W.; Bagger, A.; Schmies, H.; Kühl, S.; Rossmeisl, J.; Strasser, P. Mechanistic reaction pathways of enhanced ethylene yields during electroreduction of CO_2−CO co-feeds on Cu and Cu-tandem electrocatalysts. *Nat. Nanotechnol.* **2019**, *14*, 1063−1070.

(61) Wang, X.; Xu, A.; Li, F.; Hung, S.-F.; Nam, D.-H.; Gabardo, C. M.; Wang, Z.; Xu, Y.; Ozden, A.; Rasouli, A. S.; Ip, A. H.; Sinton, D.; Sargent, E. H. Efficient Methane Electrosynthesis Enabled by Tuning Local CO_2 Availability. *J. Am. Chem. Soc.* **2020**, *142*, 3525−3531.

(62) Jeanty, P.; Scherer, C.; Magori, E.; Wiesner-Fleischer, K.; Hinrichsen, O.; Fleischer, M. Upscaling and continuous operation of electrochemical CO_2 to CO conversion in aqueous solutions on silver gas diffusion electrodes. *J. CO2 Util.* **2018**, *24*, 454−462.

(63) Duarte, M.; De Mot, B.; Hereijgers, J.; Breugelmans, T. Electrochemical Reduction of CO_2: Effect of Convective CO_2 Supply in Gas Diffusion Electrodes. *ChemElectroChem* **2019**, *6*, 5596−5602.

(64) Endrődi, B.; Kecsenovity, E.; Samu, A.; Darvas, F.; Jones, R. V.; Török, V.; Danyi, A.; Janáky, C. Multilayer Electrolyzer Stack Converts Carbon Dioxide to Gas Products at High Pressure with High Efficiency. *ACS Energy Lett.* **2019**, *4*, 1770−1777.

(65) Dinh, C.-T.; García de Arquer, F. P.; Sinton, D.; Sargent, E. H. High Rate, Selective, and Stable Electroreduction of CO_2 to CO in Basic and Neutral Media. *ACS Energy Lett.* **2018**, *3*, 2835−2840.

(66) Dufek, E. J.; Lister, T. E.; Stone, S. G.; McIlwain, M. E. Operation of a Pressurized System for Continuous Reduction of CO_2. *J. Electrochem. Soc.* **2012**, *159*, F514−F517.

(67) Haas, T.; Krause, R.; Weber, R.; Demler, M.; Schmid, G. Technical photosynthesis involving CO_2 electrolysis and fermentation. *Nat. Catal.* **2018**, *1*, 32−39.

(68) Ma, S.; Luo, R.; Gold, J. I.; Yu, A. Z.; Kim, B.; Kenis, P. J. A. Carbon nanotube containing Ag catalyst layers for efficient and selective reduction of carbon dioxide. *J. Mater. Chem. A* **2016**, *4*, 8573−8578.

(69) Wang, R.; Haspel, H.; Pustovarenko, A.; Dikhtiarenko, A.; Russkikh, A.; Shterk, G.; Osadchii, D.; Ould-Chikh, S.; Ma, M.; Smith, W. A.; Takanabe, K.; Kapteijn, F.; Gascon, J. Maximizing Ag Utilization in High-Rate CO_2 Electrochemical Reduction with a Coordination Polymer-Mediated Gas Diffusion Electrode. *ACS Energy Lett.* **2019**, *4*, 2024−2031.

(70) Salvatore, D. A.; Weekes, D. M.; He, J.; Dettelbach, K. E.; Li, Y. C.; Mallouk, T. E.; Berlinguette, C. P. Electrolysis of Gaseous CO_2 to CO in a Flow Cell with a Bipolar Membrane. *ACS Energy Lett.* **2018**, *3*, 149−154.

(71) Edwards, J. P.; Xu, Y.; Gabardo, C. M.; Dinh, C.-T.; Li, J.; Qi, Z.; Ozden, A.; Sargent, E. H.; Sinton, D. Efficient electrocatalytic conversion of carbon dioxide in a low-resistance pressurized alkaline electrolyzer. *Appl. Energy* **2020**, *261*, 114305.

(72) Reinisch, D.; Schmid, B.; Martić, N.; Krause, R.; Landes, H.; Hanebuth, M.; Mayrhofer, K. J.; Schmid, G. Various CO_2-to-CO Electrolyzer Cell and Operation Mode Designs to avoid CO_2-

https://doi.org/10.1021/acs.iecr.1c03592
Ind. Eng. Chem. Res. XXXX, XXX, XXX−XXX

Crossover from Cathode to Anode. *Z. Phys. Chem.* **2020**, *234*, 1115−1131.
(73) Bhargava, S. S.; Proietto, F.; Azmoodeh, D.; Cofell, E. R.; Henckel, D. A.; Verma, S.; Brooks, C. J.; Gewirth, A. A.; Kenis, P. J. A. System Design Rules for Intensifying the Electrochemical Reduction of CO_2 to CO on Ag Nanoparticles. *ChemElectroChem* **2020**, *7*, 2001−2011.
(74) Lee, W. H.; Ko, Y.-J.; Choi, Y.; Lee, S. Y.; Choi, C. H.; Hwang, Y. J.; Min, B. K.; Strasser, P.; Oh, H.-S. Highly selective and scalable CO_2 to CO - Electrolysis using coral-nanostructured Ag catalysts in zero-gap configuration. *Nano Energy* **2020**, *76*, 105030.
(75) Lee, J.; Lee, W.; Ryu, K. H.; Park, J.; Lee, H.; Lee, J. H.; Park, K. T. Catholyte-free electroreduction of CO_2 for sustainable production of CO: concept, process development, techno-economic analysis, and CO_2 reduction assessment. *Green Chem.* **2021**, *23*, 2397−2410.
(76) Liu, Z.; Yang, H.; Kutz, R.; Masel, R. I. CO_2 Electrolysis to CO and O_2 at High Selectivity, Stability and Efficiency Using Sustainion Membranes. *J. Electrochem. Soc.* **2018**, *165*, J3371−J3377.
(77) Verma, S.; Hamasaki, Y.; Kim, C.; Huang, W.; Lu, S.; Jhong, H.-R. M.; Gewirth, A. A.; Fujigaya, T.; Nakashima, N.; Kenis, P. J. A. Insights into the Low Overpotential Electroreduction of CO_2 to CO on a Supported Gold Catalyst in an Alkaline Flow Electrolyzer. *ACS Energy Lett.* **2018**, *3*, 193−198.
(78) Endrődi, B.; Kecsenovity, E.; Samu, A.; Halmágyi, T.; Rojas-Carbonell, S.; Wang, L.; Yan, Y.; Janáky, C. High carbonate ion conductance of a robust PiperION membrane allows industrial current density and conversion in a zero-gap carbon dioxide electrolyzer cell. *Energy Environ. Sci.* **2020**, *13*, 4098−4105.
(79) Endrődi, B.; Samu, A.; Kecsenovity, E.; Halmágyi, T.; Sebők, D.; Janáky, C. Operando cathode activation with alkali metal cations for high current density operation of water-fed zero-gap carbon dioxide electrolysers. *Nat. Energy* **2021**, *6*, 439−448.
(80) Monteiro, M. C. O.; Philips, M. F.; Schouten, K. J. P.; Koper, M. T. M. Efficiency and selectivity of CO_2 reduction to CO on gold gas diffusion electrodes in acidic media. *Nat. Commun.* **2021**, *12*, 4943.
(81) Dinh, C.-T.; García de Arquer, F. P.; Sinton, D.; Sargent, E. H. High Rate, Selective, and Stable Electroreduction of CO_2 to CO in Basic and Neutral Media. *ACS Energy Lett.* **2018**, *3*, 2835−2840.
(82) *Produce your own Carbon Monoxide*. Haldor Topsoe. https://www.topsoe.com/processes/carbon-monoxide (accessed 2021-08-01).
(83) Keith, D. W.; Holmes, G.; St. Angelo, D.; Heidel, K. A Process for Capturing CO_2 from the Atmosphere. *Joule* **2018**, *2*, 1573−1594.
(84) Kibria Nabil, S.; McCoy, S.; Kibria, M. G. Comparative life cycle assessment of electrochemical upgrading of CO_2 to fuels and feedstocks. *Green Chem.* **2021**, *23*, 867−880.
(85) Nagahama, K.; Konishi, H.; Hoshino, D.; Hirata, M. Binary vapor-liquid equilibria of carbon dioxide-light hydrocarbons at low temperature. *J. Chem. Eng. Jpn.* **1974**, *7*, 323−328.
(86) Burr, B.; Lyddon, L. A comparison of physical solvents for acid gas removal. *Proceedings of the 87th Annual Convention of the Gas Processors Association*; Gas Processors Association: 2008; pp 100−113.
(87) Sander, R. Compilation of Henry's law constants (version 4.0) for water as solvent. *Atmos. Chem. Phys.* **2015**, *15*, 4399−4981.
(88) Benson, J.; Celin, A. Recovering Hydrogen − and Profits − from Hydrogen-Rich Offgas. *Chem. Eng. Prog.* **2018**, 55−59.
(89) Miller, G. Q.; Stoecker, J. Selection of a hydrogen separation process. *National Petroleum Refiners Association Annual Meeting*; 1989; technical paper AM-89-55.
(90) Al-Rabiah, A. A.; Timmerhaus, K. D.; Noble, R. D. Membrane Technology for Hydrogen Separation in Ethylene Plants. *The 6th World Congress of Chemical Engineering, Melbourne*; 2001; pp 1−7.
(91) Pettersen, T.; Lien, K. A new robust design model for gas separating membrane modules, based on analogy with counter-current heat exchangers. *Comput. Chem. Eng.* **1994**, *18*, 427−439.
(92) Gentry, J. C.; Solazzo, A. J. Recovery of Carboxylic Acids From Aqueous Streams. *Environ. Prog.* **1995**, *14*, 61−64.
(93) Shah, V. H.; Pham, V.; Larsen, P.; Biswas, S.; Frank, T. Liquid−Liquid Extraction for Recovering Low Margin Chemicals: Thinking beyond the Partition Ratio. *Ind. Eng. Chem. Res.* **2016**, *55*, 1731−1739.
(94) Küngas, R. Review—Electrochemical CO_2 Reduction for CO Production: Comparison of Low- and High-Temperature Electrolysis Technologies. *J. Electrochem. Soc.* **2020**, *167*, 044508.
(95) O'Brien, C. P.; Miao, R. K.; Liu, S.; Xu, Y.; Lee, G.; Robb, A.; Huang, J. E.; Xie, K.; Bertens, K.; Gabardo, C. M.; Edwards, J. P.; Dinh, C.-T.; Sargent, E. H.; Sinton, D. Single Pass CO_2 Conversion Exceeding 85% in the Electrosynthesis of Multicarbon Products via Local CO_2 Regeneration. *ACS Energy Lett.* **2021**, *6*, 2952−2959.
(96) Dutta, N.; Patil, G. Developments in CO separation. *Gas Sep. Purif.* **1995**, *9*, 277−283.
(97) Bachman, J. E.; Reed, D. A.; Kapelewski, M. T.; Chachra, G.; Jonnavittula, D.; Radaelli, G.; Long, J. R. Enabling alternative ethylene production through its selective adsorption in the metal−organic framework Mn_2(m-dobdc). *Energy Environ. Sci.* **2018**, *11*, 2423−2431.
(98) Bains, P.; Psarras, P.; Wilcox, J. CO_2 capture from the industry sector. *Prog. Energy Combust. Sci.* **2017**, *63*, 146−172.
(99) Mantripragada, H. C.; Zhai, H.; Rubin, E. S. Boundary Dam or Petra Nova − Which is a better model for CCS energy supply? *Int. J. Greenhouse Gas Control* **2019**, *82*, 59−68.
(100) Commission to the European Parliament, the Council, the European Economic and Social Committee and the Committee of the Regions. *Energy Prices and Costs in Europe*; COM/2020/951 final; European Commission: 2020; pp 1−18.
(101) EIA.*Levelized Cost of New Generation Resources in the Annual Energy Outlook*; U.S. Energy Information Administration: 2021; 25 pp.
(102) *Lazard's Levelized Cost of Energy Analysis−Version 14.0*; Lazard: 2020.
(103) *Strategic Research and Innovation Agenda: Clean Hydrogen for Europe*; Hydrogen Europe: 2020.
(104) Kvande, H.; Haupin, W. Cell voltage in aluminum electrolysis: A practical approach. *JOM* **2000**, *52*, 31−37.
(105) Kvande, H.; Haupin, W. Inert anodes for AI smelters: Energy balances and environmental impact. *JOM* **2001**, *53*, 29−33.
(106) Rosenberg, E. *Aluminium Production*; Technology Brief I10; IEA ETSAP: 2012; pp 1−5. https://iea-etsap.org/E-TechDS/PDF/I10_AlProduction_ER_March2012_Final%20GSOK.pdf
(107) Frank, W. B.; Haupin, W. E.; Vogt, H.; Bruno, M.; Thonstad, J.; Dawless, R. K.; Kvande, H.; Taiwo, O. A. *Ullmann's Encyclopedia of Industrial Chemistry*; Wiley-VCH Verlag GmbH & Co. KGaA: Weinheim, Germany, 2009; Vol. *8*, pp 255−271.
(108) Brennan, D. *Process Industry Economics: An International Perspective*; Institution of Chemical Engineers: 1998.
(109) Woods, D. R. *Rules of Thumb in Engineering Practice*; Wiley-VCH Verlag GmbH & Co. KGaA: Weinheim, Germany, 2007; pp 376−436.
(110) Barecka, M. H.; Ager, J. W.; Lapkin, A. A. Economically viable CO_2 electroreduction embedded within ethylene oxide manufacturing. *Energy Environ. Sci.* **2021**, *14*, 1530−1543.
(111) Luyben, W. L. Capital cost of compressors for conceptual design. *Chem. Eng. Process.* **2018**, *126*, 206−209.
(112) Lin, H.; He, Z.; Sun, Z.; Kniep, J.; Ng, A.; Baker, R. W.; Merkel, T. C. CO_2-selective membranes for hydrogen production and CO2 capture − Part II: Techno-economic analysis. *J. Membr. Sci.* **2015**, *493*, 794−806.
(113) Verma, S.; Lu, S.; Kenis, P. J. A. Co-electrolysis of CO_2 and glycerol as a pathway to carbon chemicals with improved technoeconomics due to low electricity consumption. *Nat. Energy* **2019**, *4*, 466−474.
(114) Khan, M. A.; Nabil, S. K.; Al-Attas, T. A.; Hu, J.; Kibria, M. G. Electrochemical Reduction of CO_2 to Ethylene with Coproduction of Glycolic Acid Via Glycerol Oxidation. *ECS Meet. Abstr.* **2021**, *MA2021-01*, 1277.

https://doi.org/10.1021/acs.iecr.1c03592
Ind. Eng. Chem. Res. XXXX, XXX, XXX−XXX

(115) van Bavel, S.; Verma, S.; Negro, E.; Bracht, M. Integrating CO_2 Electrolysis into the Gas-to-Liquids−Power-to-Liquids Process. *ACS Energy Lett.* **2020**, *5*, 2597−2601.
(116) Bienewald, F.; Leibold, E.; Tužina, P.; Roscher, G. *Ullmann's Encyclopedia of Industrial Chemistry*; Wiley-VCH Verlag GmbH & Co. KGaA: 2019; pp 1−16.
(117) Samel, U.-R.; Kohler, W.; Gamer, A. O.; Keuser, U.; Yang, S.-T.; Jin, Y.; Lin, M.; Wang, Z.; Teles, J. H. *Ullmann's Encyclopedia of Industrial Chemistry*; Wiley-VCH Verlag GmbH & Co. KGaA: Weinheim, Germany, 2018; pp 1−20.
(118) Bui, M.; Adjiman, C. S.; Bardow, A.; Anthony, E. J.; Boston, A.; Brown, S.; Fennell, P. S.; Fuss, S.; Galindo, A.; Hackett, L. A.; Hallett, J. P.; Herzog, H. J.; Jackson, G.; Kemper, J.; Krevor, S.; Maitland, G. C.; Matuszewski, M.; Metcalfe, I. S.; Petit, C.; Puxty, G.; Reimer, J.; Reiner, D. M.; Rubin, E. S.; Scott, S. A.; Shah, N.; Smit, B.; Trusler, J. P.; Webley, P.; Wilcox, J.; Mac Dowell, N. Carbon capture and storage (CCS): The way forward. *Energy Environ. Sci.* **2018**, *11*, 1062−1176.
(119) Davies, L. L.; Uchitel, K.; Ruple, J. Understanding barriers to commercial-scale carbon capture and sequestration in the United States: An empirical assessment. *Energy Policy* **2013**, *59*, 745−761.
(120) Viebahn, P.; Chappin, E. Scrutinising the Gap between the Expected and Actual Deployment of Carbon Capture and Storage—A Bibliometric Analysis. *Energies* **2018**, *11*, 2319.
(121) Akerboom, S.; Waldmann, S.; Mukherjee, A.; Agaton, C.; Sanders, M.; Kramer, G. J. Different This Time? The Prospects of CCS in the Netherlands in the 2020s. *Front. Energy Res.* **2021**, *9*, 644796.
(122) Budinis, S.; Krevor, S.; Dowell, N. M.; Brandon, N.; Hawkes, A. An assessment of CCS costs, barriers and potential. *Energy Strateg. Rev.* **2018**, *22*, 61−81.
(123) Jones, C. R.; Olfe-Kräutlein, B.; Naims, H.; Armstrong, K. The Social Acceptance of Carbon Dioxide Utilisation: A Review and Research Agenda. *Front. Energy Res.* **2017**, *5*, 11.
(124) Kant, M. Overcoming Barriers to Successfully Commercializing Carbon Dioxide Utilization. *Front. Energy Res.* **2017**, *5*, 22.
(125) Eide, L. I.; Batum, M.; Dixon, T.; Elamin, Z.; Graue, A.; Hagen, S.; Hovorka, S.; Nazarian, B.; Nøkleby, P. H.; Olsen, G. I.; Ringrose, P.; Vieira, R. A. M. Enabling Large-Scale Carbon Capture, Utilisation, and Storage (CCUS) Using Offshore Carbon Dioxide (CO_2) Infrastructure Developments−A Review. *Energies* **2019**, *12*, 1945.
(126) *Research Needs towards Sustainable Production of Fuels and Chemicals*; Nørskov, J. K., Latimer, A.; Dickens, C. F., Eds.; 2019. https://www.energy-x.eu/research-needs-report/.
(127) Eckert, M.; Fleischmann, G.; Jira, R.; Bolt, H. M.; Golka, K. *Ullmann's Encyclopedia of Industrial Chemistry*; Wiley-VCH Verlag GmbH & Co. KGaA: Weinheim, Germany, 2006; Vol. *8*, pp 255−271.
(128) Le Berre, C.; Serp, P.; Kalck, P.; Torrence, G. P. *Ullmann's Encyclopedia of Industrial Chemistry*; Wiley-VCH Verlag GmbH & Co. KGaA: Weinheim, Germany, 2014; pp 1−34.
(129) Dreher, E.-L.; Beutel, K. K.; Myers, J. D.; Lübbe, T.; Krieger, S.; Pottenger, L. H. *Ullmann's Encyclopedia of Industrial Chemistry*; Wiley-VCH Verlag GmbH & Co. KGaA: Weinheim, Germany, 2014; pp 1−81.
(130) Kosaric, N.; Duvnjak, Z.; Farkas, A.; Sahm, H.; Bringer-Meyer, S.; Goebel, O.; Mayer, D. *Ullmann's Encyclopedia of Industrial Chemistry*; Wiley-VCH Verlag GmbH & Co. KGaA: Weinheim, Germany, 2011; Vol. *44*, pp 1−72.
(131) Rebsdat, S.; Mayer, D. *Ullmann's Encyclopedia of Industrial Chemistry*; Wiley-VCH Verlag GmbH & Co. KGaA: Weinheim, Germany, 2001; Vol. *23*, pp 188−192.
(132) Zimmermann, H.; Walzl, R. *Ullmann's Encyclopedia of Industrial Chemistry*; Wiley-VCH Verlag GmbH & Co. KGaA: Weinheim, Germany, 2009; pp 465−529.
(133) Jeremic, D. *Ullmann's Encyclopedia of Industrial Chemistry*; Wiley-VCH Verlag GmbH & Co. KGaA: Weinheim, Germany, 2014; pp 1−42.
(134) Welch, V. A.; Fallon, K. J.; Gelbke, H.-P. *Ullmann's Encyclopedia of Industrial Chemistry*; Wiley-VCH Verlag GmbH & Co. KGaA: Weinheim, Germany, 2005; pp 451−464.

https://doi.org/10.1021/acs.iecr.1c03592
Ind. Eng. Chem. Res. XXXX, XXX, XXX−XXX

Supporting Information for: Electroreduction of CO_2/CO to C_2-Products: Process Modeling, Downstream Separation, System Integration, and Economic Analysis

Mahinder Ramdin,*,† Bert De Mot,‡ Andrew R. T. Morrison,¶ Tom Breugelmans,‡ Leo J. P. van den Broeke,† J. P. Martin Trusler,§ Ruud Kortlever,¶ Wiebren de Jong,¶ Othonas A. Moultos,† Penny Xiao,‖ Paul A. Webley,⊥ and Thijs J. H. Vlugt†

†*Engineering Thermodynamics, Process & Energy Department, Faculty of Mechanical, Maritime and Materials Engineering, Delft University of Technology, Leeghwaterstraat 39, 2628CB Delft, The Netherlands*

‡*Applied Electrochemistry & Catalysis, University of Antwerp, Universiteitsplein 1, 2610 Wilrijk, Belgium*

¶*Large-Scale Energy Storage, Process & Energy Department, Faculty of Mechanical, Maritime and Materials Engineering, Delft University of Technology, Leeghwaterstraat 39, 2628CB Delft, The Netherlands*

§*Imperial College London, South Kensington Campus, London SW7 2AZ, United Kingdom*

‖*Department of Chemical Engineering, University of Melbourne, Victoria 3010, Australia*

⊥*Department of Chemical Engineering, Monash University, Victoria 3800, Australia*

E-mail: m.ramdin@tudelft.nl

S1 Introduction

This supporting information contains:

- Compilation of experimental data of CO_2 reduction to C_2 products (Table S1)
- Compilation of experimental data of CO reduction to C_2 products (Table S2)
- Compilation of experimental data of CO_2 reduction to CO (Table S3)
- Capital and operating cost of the low temperature two-step tandem process (Table S4)
- Capital and operating cost of the high temperature two-step tandem process (Table S5)
- Details of the modeling of the membrane process (Section S2)
- Details of the modeling of the VPSA system for hydrogen, CO, and ethylene separation (Section S3)
- Details of the modeling of the azeotropic distillation of ethanol (Section S4)
- Details of the modeling of extraction and azeotropic distillation of acetic acid (Section S5)
- Estimation of the concentration of ethanol and acetic acid (Section S6)
- Estimation of the loss of CO_2 to (bi)carbonate (Section S7)

Table S1: Compilation of experimental data of CO_2 reduction to C2 products (ethylene, ethanol, and acetic acid).

Reactor	Voltage (V)	CD (mA/cm^2)	FE C_2H_4 (%)	FE EtOH (%)	FE AA (%)	Reference[a]
Flow cell	4	1370	60	15	5	Garcia de Arquer et al.[1]
Flow cell	NS	750	66	11	6	Dinh et al.[2]
Flow cell	2.8	300	57	1	5	De Gregorio et al.[3]
Flow cell	3	300	60	25	2	Hoang et al.[4]
Flow cell	NS	300	51	NS	NS	Vennekotter et al.[5]
Flow cell	3.7	300	38	52	2	Wang et al.[6]
Flow cell	NS	600	80	10	<1	Zhong et al.[7]
Flow cell	2	433	72	18	<1	Chen et al.[8]
Flow cell	NS	320	72	10.5	1.5	Li et al.[9]
Flow cell	NS	1600	65	12	<1	Ma et al.[10]
MEA	3.9	315	66	5	<1	Ozden et al.[11]
Flow cell	NS	670	62	NS	NS	She et al.[12]
Flow cell	NS	300	45	25	<5	Tan et al.[13]
MEA	3.7	580	70	9	8	Wang et al.[14]

[a] In some references, data was only reported in figures. Data extracted from figures are approximated.

Table S2: Compilation of experimental data of CO reduction to C2 products (ethylene, ethanol, and acetic acid).

Reactor	Voltage (V)	CD (mA/cm^2)	FE C_2H_4 (%)	FE EtOH (%)	FE AA (%)	Reference[a]
Flow cell	NS	300	55	17	10	Romero Cuellar et al.[15]
Flow cell	NS	300	45	15	9	Romero Cuellar et al.[16]
Flow cell	3.2	500	40	20	20	Jouny et al.[17]
Flow cell	NS	500	43	14	16	Jouny et al.[18]
Flow cell	NS	1250	65	18	7	Li et al.[19]
Flow cell	NS	200	16	2	48	Luc et al.[20]
MEA	2.5	160	66	6	11	Ozden et al.[21]
Flow cell	NS	200	20	10	40	Ren et al.[22]
MEA	2.3	145	35	4	30	Ripatti et al.[23]
MEA	4	700	28	5	30	Zhu et al.[24]

[a] In some references, data was only reported in figures. Data extracted from figures are approximated.

Table S3: Compilation of experimental data of CO_2 reduction to CO

Reactor configuration	Cell voltage (V)	Current density (mA/cm^2	Faraday efficiency (%)	Reference[a]
Three compartment GDE	6	150	52	Jeanty et al.[25]
Three compartment GDE	3.9	100	40	Duarte et al.[26]
Zero-gap	3	250	>90	Endrodi et al.[27]
Three compartment GDE	NS	150	>90	Dinh et al.[28]
Three compartment GDE	3.5	225	80	Dufek et al.[29]
Three compartment GDE	7.5	300	60	Haas et al.[30]
Three compartment GDE	3	350	>90	Ma et al.[31]
Zero-gap	3.8	300	96	Wang et al.[32]
Zero-gap	3.4	100	70	Salvatore et al.[33]
Micro flow cell	2.2	250	>95	Edwards et al.[34]
Three compartment GDE	NS	200	90	Reinisch et al.[35]
Flow cell	3.0	885	98	Bhargava et al.[36]
Zero-gap	3.5	350	90	Lee et al.[37]
MEA	2.2	240	93	Lee et al.[38]
MEA	2.9	100	99	Kaczur et al.[39]
MEA	3.3	600	93	Liu et al.[40]
Flow cell	2.0	100	99	Verma et al.[41]
Zero-gap	3.4	900	75	Endrodi et al.[42]
Zero-gap	3.2	470	90	Endrodi et al.[43]

[a] In some references, data was only reported in figures. Data extracted from figures are approximated.

Table S4: Capital and operating cost of the low temperature two-step tandem process

Step	CAPEX/$M	OPEX/$M/year	CAPEX/%	OPEX/%
CO_2 capture	9.5	1.4	5.2	5.7
CO_2 recycling	8.4	1.3	4.6	5.0
LT CO_2 electrolyzer	85.5	6.4	47.1	25.5
LT CO electrolyzer	59.1	13.3	32.6	52.8
C_2H_4 separation	2.3	0.1	1.3	0.4
CO/H_2 separation	0.5	0.1	0.3	0.4
Ethanol separation	6.7	0.6	3.7	2.5
Acetic acid separation	9.4	1.9	5.2	7.7
Total	181.3	25.2	100.0	100.0

Table S5: Capital and operating cost of the high temperature two-step tandem process

Step	CAPEX/$M	OPEX/$M/year	CAPEX/%	OPEX/%
CO_2 capture	9.5	1.4	7.3	5.9
CO_2 recycling	4.1	0.6	3.2	2.5
HT CO_2 electrolyzer	38.2	6.1	29.4	25.2
LT CO electrolyzer	59.1	13.3	45.5	54.9
C_2H_4 separation	2.3	0.1	1.8	0.4
CO/H_2 separation	0.5	0.1	0.4	0.4
Ethanol separation	6.7	0.6	5.2	2.6
Acetic acid separation	9.4	1.9	7.3	8.0
Total	129.8	24.2	100.0	100.0

S2 Modeling of the Membrane Process

For designing the membrane process, the counter-current hollow fiber membrane model of Pettersen and Lien[44] was used. These authors used the Patterson approximation to the logarithmic mean to formulate a simplified multicomponent model in algebraic form to explicitly calculate the permeate molar fraction ($y_{p,i}$) of a component i by:

$$y_{p,i} = \frac{-B_i + \sqrt{B_i^2 - 4A_iC_i}}{2A_i} \tag{S1}$$

where the parameters A_i, B_i, and C_i are functions of the pressure ratio (δ), the molar stage cut (θ), dimensionless permeation factor (R_i), and the feed fraction (z_i):

$$A_i = \frac{\delta}{3}\left(\frac{2\theta}{R} - \delta\right) + \frac{\theta}{3(1-\theta)}\left(\frac{\theta}{R} + \frac{\theta}{12(1-\theta)} - \delta\right) + \left(\frac{\theta}{R}\right)^2 \tag{S2}$$

$$B_i = \frac{z_i}{3}\left(1 + \frac{1}{(1-\theta)}\right)\left(\delta - \frac{\theta}{R}\right) + \frac{\theta z_i}{18(1-\theta)}\left(7 - \frac{1}{(1-\theta)}\right) \tag{S3}$$

$$C_i = \left(\frac{z_i}{6(1-\theta)}\right)^2 (\theta^2 + 12\theta - 12) \tag{S4}$$

with the pressure ratio (δ), the molar stage cut (θ), dimensionless permeation factor (R_i) defined as:

$$\delta = \frac{p_p}{p_f} \tag{S5}$$

$$\theta = \frac{n_p}{n_f} \tag{S6}$$

$$R_i = \frac{aP_ip_f}{n_f l} \tag{S7}$$

where p_p is the permeate pressure, p_f the feed pressure, n_p the molar permeate flow, n_f the molar feed flow, a the membrane area, P_i the permeability coefficient of component i, and l the membrane thickness.

The equations can be solved by applying the following constraint:

$$\sum y_{p,i} = 1 \tag{S8}$$

The selectivities and permeabilities of the different gases in polyamide membranes were taken from Al-Rabiah, see Table S6. For the separation of H_2/CO we have used polyamide A membranes, while for the separation of H_2/C_2H_4 mixtures polyamide B-H membranes were used. Note that hydrogen is the most permeable component in both membranes.

Table S6: Permeabilities and selectivities of polyamide membranes taken from Al-Rabiah.[45]

membrane	H_2/CO	H_2/CH_4	H_2/C_2H_4	H_2/C_2H_6	H_2 permeance (GPU)[a]
polyamide A	100	250	200	1000	100
polyamide B-H	56	125	250	590	500

[a] $\text{GPU} = 10^{-6}\frac{\text{cm}^3(\text{STP})}{\text{cm}^2\cdot\text{s}\cdot\text{cmHg}} = 7.501\text{x}10^{-12}\frac{\text{m}^3(\text{STP})}{\text{m}^2\cdot\text{s}\cdot\text{Pa}}$

An example calculation for the separation of hydrogen and ethylene with polyamide B-H membranes is shown in Figure S1. The calculation is based on a pressure ratio of 10, and a feed concentration of 55% hydrogen and 45% of ethylene. The figure shows that the ethylene purity increases with increasing stage cut, but it is difficult to achieve 99% purity. Furthermore, the capital cost of the membrane process increases with the purity of ethylene.

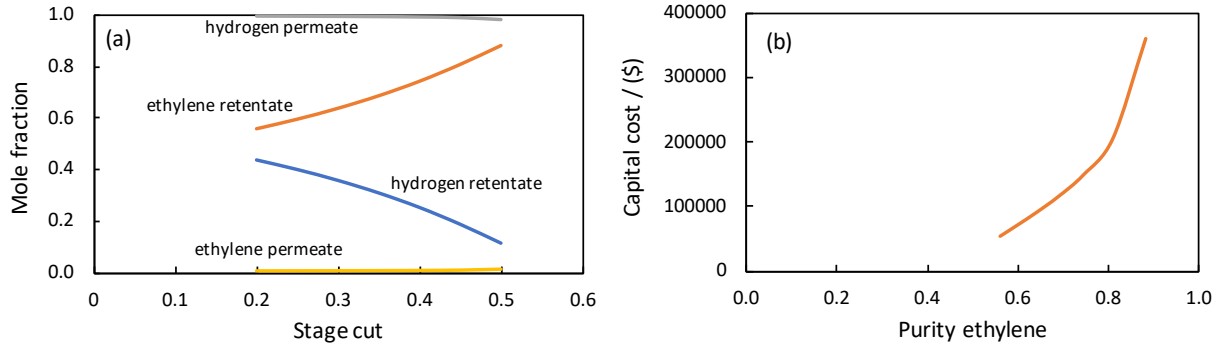

Figure S1: (a) Separation of hydrogen and ethylene with polyamide B-H membranes, and (b) capital cost of the membrane process as a function of the ethylene purity.

S3 Modeling of the VPSA process

The VPSA process for the separation of C_2H_4 and H_2 is presented in Figure S2, and the process simulation was conducted using MINSA (numerical model developed by Melbourne University).[46]

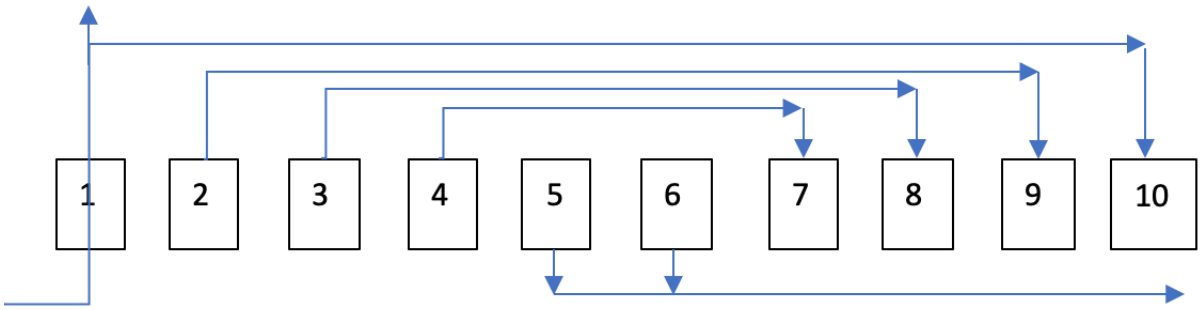

Figure S2: VPSA process design for the separation of ethylene and hydrogen. Step 1, adsorption (10 bar); Step 2 – 4, pressure equalizations; Step 7 – 9, receiving gas for re-pressurization; Step 5, blow down (1 bar); Step 6, vacuum desorption (20 kPa); and Step 10, light component re-pressurization.

The dual-site Langmuir model was used in this process to describe the adsorption capability of activated carbon:

$$q_i(P,T) = \frac{m_i B_{0i}(T) P_i}{1 + \sum B_{0i}(T) P_i} + \frac{n_i D_{0i}(T) P_i}{1 + \sum D_{0i}(T) P_i} \tag{S9}$$

where q_i is the adsorption amount for component i, m_i, n_i, B_{0i} and D_{0i} are Langmuir parameters for component i. The parameters B_{0i} and D_{0i} are correlated as:

$$B_{0i} = b_{0i} \exp\left(\frac{-Q_B}{RT}\right) \tag{S10}$$

$$D_{0i} = d_{0i} \exp\left(\frac{-Q_D}{RT}\right) \tag{S11}$$

where Q_B and Q_D represent the heat of adsorption on two different sites. The dual-site Langmuir parameters are provided in Table S7. The parameters were fitted to the experimental

data of Choi et al.[47]

Table S7: Dual-site Langmuir parameters used in the modeling of the VPSA process.

component	m_i (mol/kg)	b_{0i} (1/kPa)	Q_B (J/mol)	n_i (mol/kg)	d_{0i} (1/kPa)	Q_D (J/mol)
C_2H_4	3.4	4.29E-08	29874	3.4	4.29E-08	29874
H_2	6.39	8.76E-06	2900	6.95	1.10E-06	3000

The capital cost of the VPSA unit was estimated based on the units comprising the system (adsorbents, pressure vessels, buffer vessels, valves, vacuum pumps, and compressors). The operating cost is mainly determined by the power consumption of the vacuum pumps and compressors. The capital cost estimate of the VPSA system is provided in Table S8. The prices of different units are taken from Woods and corrected for the size, material type, pressure, and the Chemical Engineering Plant Cost Index. The correlation of Luyben[48] is used to calculate the capital cost of compressors and vacuum pumps:

$$\text{Cost (\$)} = 5840(\text{kW})^{0.82} \tag{S12}$$

The required power (kW) is calculated based on a single stage adiabatic compression assuming an isentropic efficiency of 70%.

Table S8: Capital cost estimation of the VPSA process.

Component	type	Amounts	Price/unit	Cost/M$
Adsorbent	activated carbon	6.2[a]	2000	0.01
Pressure vessels[b]	stainless steel, 1 MPa	5	157860	0.79
Compressor	centrifugal	1	563348	0.56
Vacuum pump	reciprocating	1	120255	0.12
Storage tanks	sphere, 2 bar, s/s, 100 m^3	1	645848	0.65
Valves	butterfly, 10" s/s	27	7685	0.21
Total/ M$				2.34

[a] Tons of activated carbon with a price of $2/kg. Pressure vessels are based on internal diameter of 1.2 m and height of 2 m.

S4 Modeling of Ethanol Separation

The process shown in Figure S3 was modeled in Aspen Plus using the UNIQUAC model. RADFRAC unit blocks have been used to model the distillation columns and the stripper. The optimization of the process is based on the paper of Luyben. The feed (1000 kmol/h) was assumed to contain 10 wt% ethanol with the remainder being water. The ethanol stream was concentrated up to 80 mol% in the ordinary distillation column (ODC). The ODC is optimized by using two design specifications, i.e., the purity of water in the bottom (99.99%) and the concentration of ethanol in the top (80 mol%). The design specifications were met by varying the reflux ratio and the distillate rate. The number of stages and the feed stage were optimized by reducing the reboiler duty using the Model Analysis Tool in Aspen Plus. In a similar way, the azeotropic distillation column (ADC) and the stripper were optimized. For the ADC and stripper, the purity of ethanol and water were set to 99.9% and 99.95%, respectively.

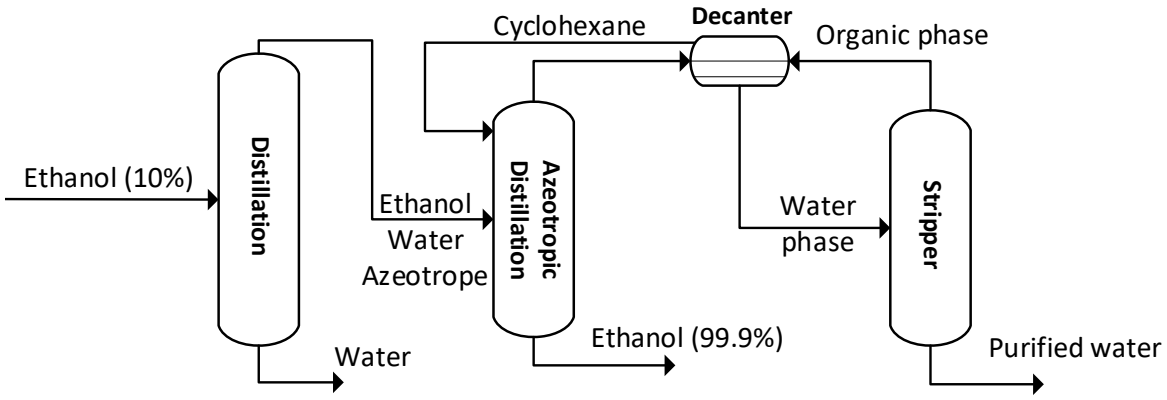

Figure S3: Azeotropic distillation of ethanol with cyclohexane. A feed with 10 wt% ethanol is introduced to a ordinary distillation column (ODC). An ethanol-water azeotropic mixture leaves the ODC as tops, while water is produced as bottoms. The near azeotropic mixture is introduced to the azeotropic distillation column (ADC), where cyclohexane is used as entrainer. Pure ethanol is obtained in the bottom of the ADC, while a cyclohexane-water-ethanol ternary azeotrope is obtained as distillate. This heterogeneous azeotropic mixture is condensed in a decanter into an organic-rich phase and an aqueous phase. The organic-rich phase is recycled to the ADC, while the water phase is sent to the stripper to produce purified water. Steam is used to strip the organics from waste water.

The cyclohexane reflux and the bottoms rate were varied to meet the design specifications of the ADC. The reboiler duty of the stripper was varied to meet the design specification (99.95% water). The optimized parameters for all the columns can be found in Table S9.

Table S9: Azeotropic distillation of ethanol using cyclohexane as entrainer.

Parameter[a]	ODC	ADC	stripper
P / bar	1	2	1
N_{stages}	30	62	11
N_{feed}	20	17	3
organic reflux (kmol/h)	-	70	-
RR (kg/kg) or RD (kW)	1.3	-	600[b]

[a] N_{stages} and N_{feed} are the number of theoretical stages and the feed stage, RR is the reflux ratio, and RD is the reboiler duty. [b] Reboiler duty

The capital and operating cost for processing 1000 kmol/h of feed containing 10 wt% (4.2 mol%) of ethanol are presented in Table xx.

Table S10: Total capital and operating costs for concentrating 10 wt% ethanol to 99.9 wt%.

Capex (M$)	Opex (M$/y)
10.2	1.3

In the electrochemical process, 6.31 mol/s (22.7 kmol/h) of ethanol is produced. If we assume that the concentration of ethanol is 10 wt% (4.2 mol%), then the total molar flow will be 541 kmol/h. We have used the six tenth rule to calculate the capital cost of this flow rate:

$$\frac{\text{Capex}_A}{\text{Capex}_B} = \left(\frac{\text{Flow}_A}{\text{Flow}_B}\right)^a \tag{S13}$$

where a is taken as 0.6. From this, a capital cost of M$7.1 is determined. The operating cost of the process is scaled linearly:

$$\text{Opex}_B = \text{Opex}_A \left(\frac{\text{Flow}_B}{\text{Flow}_A}\right) \tag{S14}$$

which gives an Opex of M$0.7/y.

S5 Modeling of Acetic Acid Separation

The process shown in Figure S4 was modeled in Aspen Plus using the NRTL-HOC model. All model parameters were taken from the Aspen database. The EXTRACT unit block was used for the extractor, and RADFRAC was used for the distillation column and the stripper. The procedure outlined in Shah et al.[49] was used to optimize the hybrid extraction-distillation process. The feed was assumed to contain 20 wt% acetic acid. The extractor was operated at 25 °C and 1 bar. The number of stages and the solvent flow in the extractor were optimized to have an FA recovery of at least 99.0%. For designing extraction columns, the extraction factor (EF) is typically set between 1.5 and 2. The EF is defined as:

$$EF = K_B \frac{S}{F} \tag{S15}$$

where K_B is the partition coefficient in Bancroft coordinates and S/F the solvent to feed ratio.

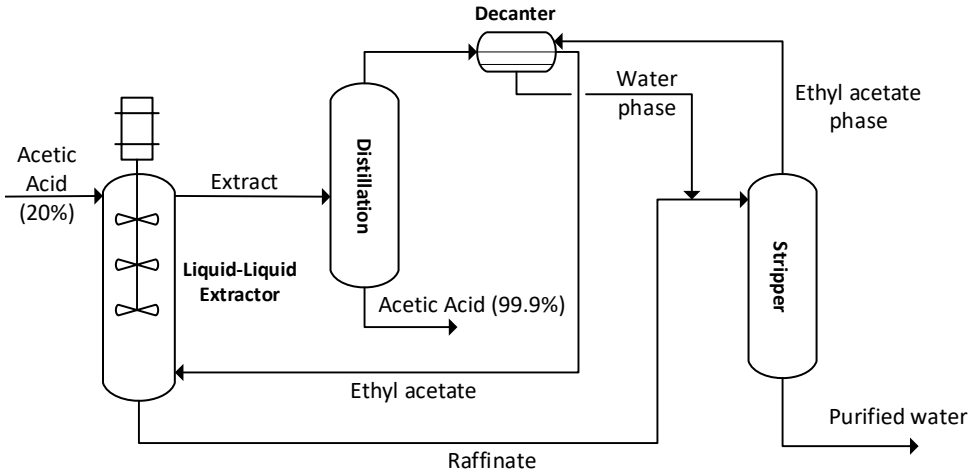

Figure S4: Hybrid extraction-distillation scheme for acetic acid separation. The feed containing 20 wt% acetic acid is introduced at the top of the extractor, while ethyl acetate solvent is fed from the bottom. The extract with acetic acid is fed to the azeotropic distillation column (ADC), which produces nearly pure acetic acid as bottoms. A water–ethyl acetate azeotropic mixture is distilled as tops in the ADC and condensed in a decanter. The organic phase from the decanter is recycled to the extractor, while the aqueous phase is combined with the raffinate and fed to the stripper. Steam is used to strip the organics from the water.

The recovery (R) is defined as:

$$R(\%) = \frac{m_{\mathrm{AA}}^{\mathrm{ext.}}}{m_{\mathrm{AA}}^{\mathrm{F}}} \tag{S16}$$

where $m_{\mathrm{AA}}^{\mathrm{ext.}}$ and $m_{\mathrm{AA}}^{\mathrm{F}}$ are the mass flow of acetic acid in the extract phase and feed, respectively. The optimized parameters for the hybrid extraction-distillation process are provided in Table S11

Table S11: Aspen Plus modeling parameters for the hybrid extraction-distillation process for acetic acid separation.

Parameter[a]	extractor	ADC	stripper
P / bar	1	1	1
N_{stages}	15	30	10
N_{feed}	1	17	1
Solvent flow (kg/h)	25000	-	-
RR (kg/kg) or RD (kW)	-	0.21	1000[b]

[a] N_{stages} and N_{feed} are the number of theoretical stages and the feed stage, RR is the reflux ratio, and RD is the reboiler duty. [b] Reboiler duty

The solvent flow is based on a feed flow of around 10233 kg/h containing 20 wt% of acetic acid. The acetic acid flow is calculated from the current density (500 mA/cm^2) and a Faraday efficiency of 20%, and an electrolyzer area of 7308 m^2. The sizing of the extractor was done using the correlations of Todd.[50] The capital cost of the extractor was then derived using the correlations of Woods,[51] see Table S12. The capital and operating costs of the distillation units were taken directly from Aspen Plus Economic Analyzer and are provided in Table S13.

Table S12: Sizing and costing of the extractor.

Sizing of extractor	
Solute	AA
Feed	water
Solvent	Ethyl acetate
Flow feed kg/hr	10233
Flow solvent kg/hr	25000
Density ρ_c (g/cm^3)	1
Density ρ_d (g/cm^3)	0.90
Flow Qc (m^3/h)	10.233
Flow Qd (m^3/h)	27.78
Ratio Qc/Qd	0.4
Constant B	0.4
Viscosity μ_c (poise)	0.01
Surface tension (dyne/cm)	30
$\Delta\rho$	0.1
Qd$^{0.5}$	5.27
$(\mu_c/\sigma)^{0.088}$	0.49
$(\rho_c^2/\mu_c\Delta\rho)^{0.138}$	2.59
Diameter D (m)	1.52
Theo. stages n	15
Height contact L (m)	17.4
Height clarif. Z (m)	3.7
Total height H (m)	21.1
Traffic flow m^3/m^2 hr	48.4
Capital cost estimation	
ref. FOB cost ($)	380000
$H * D^{1.5}$	39.54
ref $H * D^{1.5}$	10
n	0.66
L+M*	2
L/M	0.48
Cost FOB ($)	941586
L+M ($)	1883172
ref CEPCI	1000
CEPCI 2020	596.2
PM ($)	2118568
BM ($)	2965995
TM at CEPCI = 1000 ($)	4448993
Total M$	2.7

Table S13: Aspen Plus modeling parameters for the hybrid extraction-distillation process for acetic acid separation.

Unit	Capex (M$)	Opex (M$/y)
ADC and stripper	5.7	1.6
Extractor	2.7	0[a]
Total	8.4	1.6

[a] Operating cost of the extractor was neglected, since this is typically very small compared to the cost of the distillation units (ADC and stripper)

S6 Concentration of Ethanol and Acetic Acid

The concentration of liquid products depends highly on the mode of operating the the electrochemical reaction. For example, in the zero-gap mode more concentrated products can be obtained than in a flowing electrolyte cell. We will show some sample calculations to estimate the concentrations of ethanol and acetic acid in different cell configuration. The calculations are based on a current density of 500 mA/cm^2 and a Faraday efficiency of 50% for ethylene, 20% for ethanol, 20% for acetic acid, and 10% for hydrogen. From these assumptions and the constraint that we need to convert 10 ton/h of CO_2 to C_2 products (for which an electrolyzer area of 7308 m^2 is required), it is possible to calculate the production rate of ethanol (6.3 mol/s) and acetic acid (9.5 mol/s). The concentration of both products now depends on the supply rate of water to the cathode compartment. In lab experiments, typically a water flow of 0.01–2 ml/min·cm^2 is used. For 0.01, 0.1, and 1 ml/min·cm^2, an ethanol concentration of respectively 0.9%, 0.09%, and 0.009% is obtained. It is clear that low concentration of ethanol will be obtained in a cell with flowing electrolytes.

In the zero-gap mode higher concentration can be obtained, because very low amounts of water are supplied to the cathode. The amount of water in saturated CO_2 can be obtained from the equilibrium relations:[52]

$$y_{CO_2} P = x_{CO_2} H_{CO_2} \quad \text{(Henry's law)} \tag{S17}$$

$$y_w = x_w P_w^{\text{sat.}} \quad \text{(Raoult's law)} \tag{S18}$$

where P is the total pressure, H_{CO_2} the Henry constant of CO_2 in water, y_{CO_2} and y_w the gas phase composition of CO_2 and water, x_{CO_2} and x_w the liquid phase composition of CO_2 and water, and $P_w^{\text{sat.}}$ the saturated vapor pressure of water. The Henry constant of CO_2 in water as a function of temperature is taken from the literature:[53]

$$\ln(H_{CO_2}/\text{MPa}) = -6.8346 + \frac{1.2817 \cdot 10^4}{T} + \frac{3.7668 \cdot 10^6}{T^2} + \frac{2.997 \cdot 10^8}{T^3} \tag{S19}$$

where the Henry constant is in MPa and the temperature in Kelvin. The saturated vapor pressure of water is obtained from the Antoine equation:[54]

$$P_w^{\text{sat.}} = 10^{A-\frac{B}{C+T}} \tag{S20}$$

where $P_w^{\text{sat.}}$ is in mmHg (760 mmHg = 101.325 kPa) and T in °C. The constant A, B, and C are 8.07131, 1730.63, and 233.426, respectively.[55] By combining the equilibrium relations and setting the total pressure to 1 bar, one can obtain the solubility of CO_2 in water (x_{CO_2}):

$$y_{CO_2}P + y_wP = x_{CO_2}H_{CO_2} + x_wP_w^{\text{sat.}} \tag{S21}$$

In this equation the only unknown is x_{CO_2}, since ($y_{CO_2} + y_w = 1$) and $x_w = (1 - x_{CO_2})$. The amount of water in the gas phase can then be obtained from Raoult's law. The composition of water in the gas phase at 25 °C is around $2.1{\cdot}10^{-5}$ mole fraction. Thus, $2.1{\cdot}10^{-5}$ moles of water per mole of CO_2 is supplied to the cathode. If we assume that this amount of water will mix with the produced ethanol, then the ethanol concentration will be very high (>99.9%). In practice, such a high ethanol concentration is not achieved in zero-gap electrolyzers due to water transport from the anolyte to the catholyte, which dilutes the product stream. To calculate the ethanol concentration accurately, a more complex water balance of the cathode compartment should be solved. The transport of water due to electro-osmotic drag and diffusion, and consumption of water due to electrochemical reactions need to be considered.

The concentration of acetic acid depends on the flow rate of water in the center compartment of the 3-compartment cell. At a current density of 500 mA/cm^2 and a Faraday efficiency of 20%, around 9.5 mol/s of acetate is produced. Therefore, the water flow in the center compartment should be around 2.3 kg/s to obtain 20 wt% of acetic acid. Note that we have assumed that all acetate produced in the cathode compartment is transported to the center compartment.

S7 Loss of CO_2 to (Bi)carbonate

The amount of CO_2 that is lost due to (bi)carbonate formation is estimated from the OH^- generation. We have assumed that all OH^- generated in the CO2RR and water reduction will react with CO_2 to produce (bi)carbonate.

$$2CO_2 + 8H_2O + 12e^- \leftrightarrow C_2H_4 + 12OH^- \tag{S22}$$

$$2CO_2 + 9H_2O + 12e^- \leftrightarrow C_2H_5OH + 12OH^- \tag{S23}$$

$$2CO_2 + 6H_2O + 8e^- \leftrightarrow CH_3COOH + 8OH^- \tag{S24}$$

$$2H_2O + 2e^- \leftrightarrow H_2 + 2OH^- \tag{S25}$$

For every mole of ethylene, ethanol, acetic acid, and hydrogen 12, 12, 8, and 2 moles of hydroxide ions are produced. The hydroxide ions will react with CO_2:

$$CO_2 + OH^- \leftrightarrow HCO_3^- \tag{S26}$$

For a current density of 500 mA/cm^2 and a Faraday efficiency of 50% for ethylene, 20% for ethanol, 20% for acetic acid, and 10% for hydrogen, 6 times more CO_2 (60 ton/h) is lost than electrochemically converted (10 ton/h) to C_2 products. It is clear that the cost of CO_2 will increase dramatically if the CO2RR is performed in alkaline media. Note that we have only accounted for CO_2 reactions with the hydroxides generated from the electrochemical reduction of CO_2 and water. More CO_2 will be lost if an alkaline catholyte (e.g., KOH) is used. In the process design, we have assumed that all the lost CO_2 (in the form of (bi)carbonate) can be regenerated in the center compartment of a 3-compartment cell.

References

(1) García de Arquer, F. P.; Dinh, C.-T.; Ozden, A.; Wicks, J.; McCallum, C.; Kirmani, A. R.; Nam, D.-H.; Gabardo, C.; Seifitokaldani, A.; Wang, X.; Li, Y. C.; Li, F.; Edwards, J.; Richter, L. J.; Thorpe, S. J.; Sinton, D.; Sargent, E. H. CO_2 electrolysis to multicarbon products at activities greater than 1 A cm^{-2}. *Science* **2020**, *367*, 661–666.

(2) Dinh, C.-T.; Burdyny, T.; Kibria, M. G.; Seifitokaldani, A.; Gabardo, C. M.; García de Arquer, F. P.; Kiani, A.; Edwards, J. P.; De Luna, P.; Bushuyev, O. S.; Zou, C.; Quintero-Bermudez, R.; Pang, Y.; Sinton, D.; Sargent, E. H. CO_2 electroreduction to ethylene via hydroxide-mediated copper catalysis at an abrupt interface. *Science* **2018**, *360*, 783–787.

(3) De Gregorio, G. L.; Burdyny, T.; Loiudice, A.; Iyengar, P.; Smith, W. A.; Buonsanti, R. Facet-Dependent Selectivity of Cu Catalysts in Electrochemical CO_2 Reduction at Commercially Viable Current Densities. *ACS Catal.* **2020**, *10*, 4854–4862.

(4) Hoang, T. T. H.; Verma, S.; Ma, S.; Fister, T. T.; Timoshenko, J.; Frenkel, A. I.; Kenis, P. J. A.; Gewirth, A. A. Nanoporous Copper–Silver Alloys by Additive-Controlled Electrodeposition for the Selective Electroreduction of CO_2 to Ethylene and Ethanol. *J. Am. Chem. Soc.* **2018**, *140*, 5791–5797.

(5) Vennekötter, J.-B.; Scheuermann, T.; Sengpiel, R.; Wessling, M. The electrolyte matters: Stable systems for high rate electrochemical CO_2 reduction. *J. CO2 Util.* **2019**, *32*, 202–213.

(6) Wang, X.; Wang, Z.; García de Arquer, F. P.; Dinh, C.-T.; Ozden, A.; Li, Y. C.; Nam, D.-H.; Li, J.; Liu, Y.-S.; Wicks, J.; Chen, Z.; Chi, M.; Chen, B.; Wang, Y.; Tam, J.; Howe, J. Y.; Proppe, A.; Todorović, P.; Li, F.; Zhuang, T.-T.; Gabardo, C. M.; Kirmani, A. R.; McCallum, C.; Hung, S.-F.; Lum, Y.; Luo, M.; Min, Y.; Xu, A.;

O'Brien, C. P.; Stephen, B.; Sun, B.; Ip, A. H.; Richter, L. J.; Kelley, S. O.; Sinton, D.; Sargent, E. H. Efficient electrically powered CO_2-to-ethanol via suppression of deoxygenation. *Nat. Energy* **2020**, *5*, 478–486.

(7) Zhong, M.; Tran, K.; Min, Y.; Wang, C.; Wang, Z.; Dinh, C.-T.; De Luna, P.; Yu, Z.; Rasouli, A. S.; Brodersen, P.; Sun, S.; Voznyy, O.; Tan, C.-S.; Askerka, M.; Che, F.; Liu, M.; Seifitokaldani, A.; Pang, Y.; Lo, S.-C.; Ip, A.; Ulissi, Z.; Sargent, E. H. Accelerated discovery of CO_2 electrocatalysts using active machine learning. *Nature* **2020**, *581*, 178–183.

(8) Chen, X.; Chen, J.; Alghoraibi, N. M.; Henckel, D. A.; Zhang, R.; Nwabara, U. O.; Madsen, K. E.; Kenis, P. J. A.; Zimmerman, S. C.; Gewirth, A. A. Electrochemical CO_2-to-ethylene conversion on polyamine-incorporated Cu electrodes. *Nat. Catal.* **2021**, *4*, 20–27.

(9) Li, F.; Thevenon, A.; Rosas-Hernández, A.; Wang, Z.; Li, Y.; Gabardo, C. M.; Ozden, A.; Dinh, C. T.; Li, J.; Wang, Y.; Edwards, J. P.; Xu, Y.; McCallum, C.; Tao, L.; Liang, Z.-Q.; Luo, M.; Wang, X.; Li, H.; O'Brien, C. P.; Tan, C.-S.; Nam, D.-H.; Quintero-Bermudez, R.; Zhuang, T.-T.; Li, Y. C.; Han, Z.; Britt, R. D.; Sinton, D.; Agapie, T.; Peters, J. C.; Sargent, E. H. Molecular tuning of CO_2-to-ethylene conversion. *Nature* **2020**, *577*, 509–513.

(10) Ma, W.; Xie, S.; Liu, T.; Fan, Q.; Ye, J.; Sun, F.; Jiang, Z.; Zhang, Q.; Cheng, J.; Wang, Y. Electrocatalytic reduction of CO_2 to ethylene and ethanol through hydrogen-assisted C–C coupling over fluorine-modified copper. *Nat. Catal.* **2020**, *3*, 478–487.

(11) Ozden, A.; Li, F.; Garcia de Arquer, F. P.; Rosas-Hernández, A.; Thevenon, A.; Wang, Y.; Hung, S.-F.; Wang, X.; Chen, B.; Li, J.; Wicks, J.; Luo, M.; Wang, Z.; Agapie, T.; Peters, J. C.; Sargent, E. H.; Sinton, D. High-Rate and Efficient Ethylene

Electrosynthesis Using a Catalyst/Promoter/Transport Layer. *ACS Energy Lett.* **2020**, *5*, 2811–2818.

(12) She, X.; Zhang, T.; Li, Z.; Li, H.; Xu, H.; Wu, J. Tandem Electrodes for Carbon Dioxide Reduction into C2+ Products at Simultaneously High Production Efficiency and Rate. *Cell Reports Phys. Sci.* **2020**, *1*, 100051.

(13) Tan, Y. C.; Lee, K. B.; Song, H.; Oh, J. Modulating Local CO_2 Concentration as a General Strategy for Enhancing C-C Coupling in CO_2 Electroreduction. *Joule* **2020**, *4*, 1104–1120.

(14) Wang, Y.; Wang, Z.; Dinh, C.-T.; Li, J.; Ozden, A.; Golam Kibria, M.; Seifitokaldani, A.; Tan, C.-S.; Gabardo, C. M.; Luo, M.; Zhou, H.; Li, F.; Lum, Y.; McCallum, C.; Xu, Y.; Liu, M.; Proppe, A.; Johnston, A.; Todorovic, P.; Zhuang, T.-T.; Sinton, D.; Kelley, S. O.; Sargent, E. H. Catalyst synthesis under CO_2 electroreduction favours faceting and promotes renewable fuels electrosynthesis. *Nat. Catal.* **2020**, *3*, 98–106.

(15) Romero Cuellar, N.; Wiesner-Fleischer, K.; Fleischer, M.; Rucki, A.; Hinrichsen, O. Advantages of CO over CO_2 as reactant for electrochemical reduction to ethylene, ethanol and n-propanol on gas diffusion electrodes at high current densities. *Electrochim. Acta* **2019**, *307*, 164–175.

(16) Romero Cuellar, N.; Scherer, C.; Kaçkar, B.; Eisenreich, W.; Huber, C.; Wiesner-Fleischer, K.; Fleischer, M.; Hinrichsen, O. Two-step electrochemical reduction of CO_2 towards multi-carbon products at high current densities. *J. CO2 Util.* **2020**, *36*, 263–275.

(17) Jouny, M.; Luc, W.; Jiao, F. High-rate electroreduction of carbon monoxide to multicarbon products. *Nat. Catal.* **2018**, *1*, 748–755.

(18) Jouny, M.; Lv, J.-J.; Cheng, T.; Ko, B. H.; Zhu, J.-J.; Goddard, W. A.; Jiao, F. Formation of carbon–nitrogen bonds in carbon monoxide electrolysis. *Nat. Chem.* **2019**, *11*, 846–851.

(19) Li, J.; Wang, Z.; McCallum, C.; Xu, Y.; Li, F.; Wang, Y.; Gabardo, C. M.; Dinh, C.-t.; Zhuang, T.-t.; Wang, L.; Howe, J. Y.; Ren, Y.; Sargent, E. H.; Sinton, D. Constraining CO coverage on copper promotes high-efficiency ethylene electroproduction. *Nat. Catal.* **2019**, *2*, 1124–1131.

(20) Luc, W.; Fu, X.; Shi, J.; Lv, J.-J.; Jouny, M.; Ko, B. H.; Xu, Y.; Tu, Q.; Hu, X.; Wu, J.; Yue, Q.; Liu, Y.; Jiao, F.; Kang, Y. Two-dimensional copper nanosheets for electrochemical reduction of carbon monoxide to acetate. *Nat. Catal.* **2019**, *2*, 423–430.

(21) Ozden, A.; Wang, Y.; Li, F.; Luo, M.; Sisler, J.; Thevenon, A.; Rosas-Hernández, A.; Burdyny, T.; Lum, Y.; Yadegari, H.; Agapie, T.; Peters, J. C.; Sargent, E. H.; Sinton, D. Cascade CO_2 electroreduction enables efficient carbonate-free production of ethylene. *Joule* **2021**, *5*, 706–719.

(22) Ren, S.; Fink, A. G.; Lees, E. W.; Zhang, Z.; Wu, W.; Dvorak, D. J. Molecular electrocatalysts transform CO into C2+ products effectively in a flow cell. *Researchsquare.Com* **2020**, 1–18.

(23) Ripatti, D. S.; Veltman, T. R.; Kanan, M. W. Carbon Monoxide Gas Diffusion Electrolysis that Produces Concentrated C_2 Products with High Single-Pass Conversion. *Joule* **2019**, *3*, 240–256.

(24) Zhu, P.; Xia, C.; Liu, C.-Y.; Jiang, K.; Gao, G.; Zhang, X.; Xia, Y.; Lei, Y.; Alshareef, H. N.; Senftle, T. P.; Wang, H. Direct and continuous generation of pure acetic acid solutions via electrocatalytic carbon monoxide reduction. *Proc. Natl. Acad. Sci.* **2021**, *118*, e2010868118.

(25) Jeanty, P.; Scherer, C.; Magori, E.; Wiesner-Fleischer, K.; Hinrichsen, O.; Fleischer, M. Upscaling and continuous operation of electrochemical CO_2 to CO conversion in aqueous solutions on silver gas diffusion electrodes. *J. CO2 Util.* **2018**, *24*, 454–462.

(26) Duarte, M.; De Mot, B.; Hereijgers, J.; Breugelmans, T. Electrochemical Reduction of CO_2 : Effect of Convective CO_2 Supply in Gas Diffusion Electrodes. *ChemElectroChem* **2019**, *6*, 5596–5602.

(27) Endrődi, B.; Kecsenovity, E.; Samu, A.; Darvas, F.; Jones, R. V.; Török, V.; Danyi, A.; Janáky, C. Multilayer Electrolyzer Stack Converts Carbon Dioxide to Gas Products at High Pressure with High Efficiency. *ACS Energy Lett.* **2019**, *4*, 1770–1777.

(28) Dinh, C.-T.; García de Arquer, F. P.; Sinton, D.; Sargent, E. H. High Rate, Selective, and Stable Electroreduction of CO_2 to CO in Basic and Neutral Media. *ACS Energy Lett.* **2018**, *3*, 2835–2840.

(29) Dufek, E. J.; Lister, T. E.; Stone, S. G.; McIlwain, M. E. Operation of a Pressurized System for Continuous Reduction of CO_2. *J. Electrochem. Soc.* **2012**, *159*, F514–F517.

(30) Haas, T.; Krause, R.; Weber, R.; Demler, M.; Schmid, G. Technical photosynthesis involving CO_2 electrolysis and fermentation. *Nat. Catal.* **2018**, *1*, 32–39.

(31) Ma, S.; Luo, R.; Gold, J. I.; Yu, A. Z.; Kim, B.; Kenis, P. J. A. Carbon nanotube containing Ag catalyst layers for efficient and selective reduction of carbon dioxide. *J. Mater. Chem. A* **2016**, *4*, 8573–8578.

(32) Wang, R.; Haspel, H.; Pustovarenko, A.; Dikhtiarenko, A.; Russkikh, A.; Shterk, G.; Osadchii, D.; Ould-Chikh, S.; Ma, M.; Smith, W. A.; Takanabe, K.; Kapteijn, F.; Gascon, J. Maximizing Ag Utilization in High-Rate CO_2 Electrochemical Reduction with a Coordination Polymer-Mediated Gas Diffusion Electrode. *ACS Energy Lett.* **2019**, *4*, 2024–2031.

(33) Salvatore, D. A.; Weekes, D. M.; He, J.; Dettelbach, K. E.; Li, Y. C.; Mallouk, T. E.; Berlinguette, C. P. Electrolysis of Gaseous CO_2 to CO in a Flow Cell with a Bipolar Membrane. *ACS Energy Lett.* **2018**, *3*, 149–154.

(34) Edwards, J. P.; Xu, Y.; Gabardo, C. M.; Dinh, C.-T.; Li, J.; Qi, Z.; Ozden, A.; Sargent, E. H.; Sinton, D. Efficient electrocatalytic conversion of carbon dioxide in a low-resistance pressurized alkaline electrolyzer. *Appl. Energy* **2020**, *261*, 114305.

(35) Reinisch, D.; Schmid, B.; Martić, N.; Krause, R.; Landes, H.; Hanebuth, M.; Mayrhofer, K. J.; Schmid, G. Various CO_2-to-CO Electrolyzer Cell and Operation Mode Designs to avoid CO_2-Crossover from Cathode to Anode. *Zeitschrift für Phys. Chemie* **2020**, *234*, 1115–1131.

(36) Bhargava, S. S.; Proietto, F.; Azmoodeh, D.; Cofell, E. R.; Henckel, D. A.; Verma, S.; Brooks, C. J.; Gewirth, A. A.; Kenis, P. J. A. System Design Rules for Intensifying the Electrochemical Reduction of CO_2 to CO on Ag Nanoparticles. *ChemElectroChem* **2020**, *7*, 2001–2011.

(37) Lee, W. H.; Ko, Y.-J.; Choi, Y.; Lee, S. Y.; Choi, C. H.; Hwang, Y. J.; Min, B. K.; Strasser, P.; Oh, H.-S. Highly selective and scalable CO_2 to CO - Electrolysis using coral-nanostructured Ag catalysts in zero-gap configuration. *Nano Energy* **2020**, *76*, 105030.

(38) Lee, J.; Lee, W.; Ryu, K. H.; Park, J.; Lee, H.; Lee, J. H.; Park, K. T. Catholyte-free electroreduction of CO_2 for sustainable production of CO: concept, process development, techno-economic analysis, and CO_2 reduction assessment. *Green Chem.* **2021**, *23*, 2397–2410.

(39) Kaczur, J. J.; Yang, H.; Liu, Z.; Sajjad, S. D.; Masel, R. I. Carbon Dioxide and Water Electrolysis Using New Alkaline Stable Anion Membranes. *Front. Chem.* **2018**, *6*, 1–16.

(40) Liu, Z.; Yang, H.; Kutz, R.; Masel, R. I. CO_2 Electrolysis to CO and O_2 at High Selectivity, Stability and Efficiency Using Sustainion Membranes. *J. Electrochem. Soc.* **2018**, *165*, J3371–J3377.

(41) Verma, S.; Hamasaki, Y.; Kim, C.; Huang, W.; Lu, S.; Jhong, H.-R. M.; Gewirth, A. A.; Fujigaya, T.; Nakashima, N.; Kenis, P. J. A. Insights into the Low Overpotential Electroreduction of CO_2 to CO on a Supported Gold Catalyst in an Alkaline Flow Electrolyzer. *ACS Energy Lett.* **2018**, *3*, 193–198.

(42) Endrődi, B.; Kecsenovity, E.; Samu, A.; Halmágyi, T.; Rojas-Carbonell, S.; Wang, L.; Yan, Y.; Janáky, C. High carbonate ion conductance of a robust PiperION membrane allows industrial current density and conversion in a zero-gap carbon dioxide electrolyzer cell. *Energy Environ. Sci.* **2020**, *13*, 4098–4105.

(43) Endrődi, B.; Samu, A.; Kecsenovity, E.; Halmágyi, T.; Sebők, D.; Janáky, C. Operando cathode activation with alkali metal cations for high current density operation of water-fed zero-gap carbon dioxide electrolysers. *Nat. Energy* **2021**, *6*, 439–448.

(44) Pettersen, T.; Lien, K. A new robust design model for gas separating membrane modules, based on analogy with counter-current heat exchangers. *Comput. Chem. Eng.* **1994**, *18*, 427–439, An International Journal of Computer Applications in Chemical Engineering.

(45) Al-Rabiah, a. a.; Timmerhaus, K. D.; Noble, R. D. Membrane Technology for Hydrogen Separation in Ethylene Plants. 6th World Congr. Chem. Eng. Melbourne, 2001; pp 1–7.

(46) Xiao, P.; Zhang, J.; Webley, P.; Li, G.; Singh, R.; Todd, R. Capture of CO_2 from flue gas streams with zeolite 13X by vacuum-pressure swing adsorption. *Adsorption* **2008**, *14*, 575–582.

(47) Choi, B.-U.; Choi, D.-K.; Lee, Y.-W.; Lee, B.-K.; Kim, S.-H. Adsorption Equilibria of

Methane, Ethane, Ethylene, Nitrogen, and Hydrogen onto Activated Carbon. *J. Chem. Eng. Data* **2003**, *48*, 603–607.

(48) Luyben, W. L. Capital cost of compressors for conceptual design. *Chemical Engineering and Processing - Process Intensification* **2018**, *126*, 206–209.

(49) Shah, V. H.; Pham, V.; Larsen, P.; Biswas, S.; Frank, T. Liquid–Liquid Extraction for Recovering Low Margin Chemicals: Thinking beyond the Partition Ratio. *Ind. Eng. Chem. Res.* **2016**, *55*, 1731–1739.

(50) Todd, D. B. *Ferment. Biochem. Eng. Handb.*, 2nd ed.; Elsevier, 2014; pp 225–238.

(51) Woods, D. R. *Rules of Thumb in Engineering Practice*; Wiley-VCH Verlag GmbH & Co. KGaA: Weinheim, Germany, 2007; pp 376–436.

(52) Smith, J.; Van Ness, H.; Abbott, M. *Introduction to Chemical Engineering Thermodynamics*, seventh ed.; CHEMICAL ENGINEERING SERIES; McGraw-Hill Education: New York, 2005.

(53) Carroll, J. J.; Slupsky, J. D.; Mather, A. E. The Solubility of Carbon Dioxide in Water at Low Pressure. *J. Phys. Chem. Ref. Data* **1991**, *20*, 1201–1209.

(54) Prausnitz, J.; Lichtenthaler, R.; Gomes de Azevedo, E. *Molecular thermodynamics of fluid-phase equilibria*, 3rd ed.; Prentice Hall PTR: New York, 1999.

(55) Dortmund Data Bank, url = www.ddbst.com, note = Accessed: 2021-08-01.